DUPLICATE ALSO (266)

# Long-Range Forecasting and Climate Research

## The Climate of the World

### 6. The El Nino/Southern Oscillation, The Quasi-Biennial Oscillation and the 30-60 Day Variations

by

C. K. Folland and D. E. Parker

LRFC 25

July 1988

ORGS UKMO L

National Meteorological Library
FitzRoy Road, Exeter, Devon. EX1 3PB

FH16

DUPLICATE ALSO

METEOROLOGICAL OFFICE
152.1
15 AUG 1988
LIBRARY

LONG RANGE FORECASTING AND
CLIMATE RESEARCH MEMORANDUM NO. 25
(LRFC 25)

# THE CLIMATE OF THE WORLD
# 6. THE EL NINO/SOUTHERN OSCILLATION, THE QUASI-BIENNIAL OSCILLATION, AND THE 30-60 DAY VARIATIONS

by

C K FOLLAND AND D E PARKER

NOTES ON AN ADVANCED LECTURE FOR
THE SCIENTIFIC OFFICERS' COURSE,
METEOROLOGICAL OFFICE 1988

Met O 13 (Synoptic Climatology Branch)
Meteorological Office
London Road
Bracknell
Berkshire RG12 2SZ

July 1988

Note. This paper has not been published. Permission to quote from it should be obtained from the Assistant Director (Synoptic Climatology) Meteorological Office.

LONDON, METEOROLOGICAL OFFICE.
Long-Range Forecasting and Climate
Research Memorandum No.25

The climate of the world.
6. The El Nino/Southern Oscillation, the
quasi-biennial oscillation and the 30-60 day
variations.

00160988 FH1B

This Memorandum is the fourth is a series of six on:

# THE CLIMATE OF THE WORLD

BY

C K FOLLAND AND D E PARKER

Based on ten Advanced Lectures for the Scientific Officers' Course 1988, and one Advanced Lecture delivered by D J Carson in March 1982.

## INDEX TO SERIES


| | | |
|---|---|---|
| LRFC22 | 1. | INTRODUCTION TO WORLD CLIMATE |
| | 2. | DESCRIPTION OF WORLD CLIMATE<br>(Advanced Lectures 1 and 2). C K Folland and D E Parker |
| LRFC23 | 3. | CLIMATIC FORCING AND FEEDBACK PROCESSES. I. FORCING FROM ABOVE |
| | 4. | CLIMATIC FORCING AND FEEDBACK PROCESSES. II. INTERACTIONS WITH THE LAND SURFACE<br>(Advanced Lectures 3 and 4). C K Folland and D E Parker |
| LRFC24 | 5. | OCEAN ATMOSPHERE INTERACTION<br>(Advanced Lecture 5). D E Parker and C K Folland. |
| LRFC25 | 6. | THE EL NINO/SOUTHERN OSCILLATION, THE QUASI-BIENNIAL OSCILLATION, AND THE 30-60 DAY VARIATIONS.<br>(Advanced Lecture 6). C K Folland and D E Parker. |
| LRFC26 | 7. | A REVIEW OF PALAEOCLIMATE FROM THE EARLY EARTH TO THE PLEISTOCENE ICE AGES. |
| | 8. | CLIMATE FROM THE LATE GLACIAL TO THE "LITTLE ICE AGE"<br>(Advanced Lectures 7 and 8). C K Folland and D E Parker. |
| LRFC27 | 9. | CLIMATIC CHANGE IN THE INSTRUMENTAL PERIOD<br>(Advanced Lecture 9). D E Parker and C K Folland. |
| LRFC28 | 10. | CARBON DIOXIDE AND OTHER GREENHOUSE CASES, AND CLIMATIC VARIATION (WITH APPENDIX ON SIMPLE CLIMATE MODELS)<br>(Advanced Lecture 10 plus an Advanced Lecture delivered by D J Carson in March 1982). D E Parker, C K Folland and D J Carson |

ADVANCED LECTURE NO 6

# THE EL NINO/SOUTHERN OSCILLATION, THE QUASI-BIENNIAL OSCILLATION, AND THE 30-60 DAY VARIATIONS.

C K FOLLAND AND D E PARKER

MET O 13

SUMMARY

The El Nino-Southern Oscillation phenomenon is a well-known example of ocean-atmosphere interaction, involving not only marked changes of sea-surface temperature and atmospheric circulation and rainfall in the equatorial Pacific, but also related changes in the atmosphere and ocean throughout the remainder of the tropics, and in higher latitudes particularly in the Pacific-North America section. A review is given of observational and numerical modelling studies of El Nino-Southern Oscillation, and the mechanisms involved are discussed. Recent attempts to predict its oceanographic component are included. A briefer consideration is given to the Quasi-biennial Oscillation of winds and temperatures in the equatorial lower stratosphere. Theoretical models, which explain the Quasi-biennial Oscillation in terms of absorption of vertically-propagating waves, are described. Finally, we present an account of the variations on the 30-60 day timescale, which are especially important in the tropics.

## 6.1 - THE EL NINO - SOUTHERN OSCILLATION (ENSO)

### 6.1.1 Introduction

The term El Nino (The "Christ Child") was originally given to a weak warm coastal current which commences around Christmas and flows southwards along the coast of Ecuador and Peru during each Southern Hemisphere summer. Every few years the near-coastal warming associated with the current becomes particularly intense (4-7°C); during (usually) the following 12 months the surface of the entire Central and Eastern tropical Pacific Ocean is typically 1-3°C warmer than normal. In December 1982, the sea surface temperature in the open ocean near 5°S, 130°W, was almost 6°C above normal, an amount which can usefully be compared with the annual cycle of sea surface temperature for the world shown in Lecture 5, Fig 5.1.

Fig 6.1A shows the observed sea surface temperature in the Pacific and Fig 6.1B the observed sea surface temperature anomaly (SSTA) there during the Northern Hemisphere winter of 1982-83, near the most intense phase of one of these tropical Pacific warmings (Quiroz (1983)). The term 'El Nino' is now generally used by climatologists to describe the widespread oceanic warming and not the local coastal warming. Fig 2.5, Lecture 2, showed mean January SST for 1951-80; it can be seen that the normal east-west gradient of tropical Pacific SST has nearly disappeared in Fig 6.1A and that the absolute maximum SST in the period Dec 1982 to Feb 1983 was placed about 60°E of its normal position. The 1982-83 El Nino will be discussed below; Quiroz gives a very good observational account.

High surface temperatures are only one aspect of the anomalous behaviour of the tropical Pacific Ocean during an El Nino: the entire thermal and dynamic structure of the upper ocean is different from normal (Gill and Rasmusson (1983)). The presence of such a large anomalous heat source at the lower boundary of the tropical atmosphere can also be expected to affect the atmospheric general circulation and it became clear about 20 years ago that a near global scale mean sea-level pressure (PMSL) sea-saw known for over half a century as the Southern Oscillation (SO) is linked to El Nino.

The possible existence of a large-scale interannual PMSL fluctuation was first hinted at by a Swede, Hildebrandsson in 1897 who found an out of phase relationship between PMSL at Sydney, Australia and Buenos Aires, Argentina. In 1902-6 Lockyer and Lockyer uncovered the worldwide scale of the PMSL fluctuation, but Walker and Bliss (1923-37) provided the first detailed analyses of the companion temperature and rainfall fluctuations and were the first to name the phenomenon the "Southern Oscillation". See Rasmusson and Carpenter (RC) (1982) for historical detail. Fig 6.2A shows the correlation between annual PMSL anomalies at Easter Island and many other stations distributed worldwide, produced by Berlage and de Boer (1959), and confirmed several times since Berlage and de Boer's paper. Djakarta, Java and Easter Island are 140° of longitude (15,000 km) apart and all investigations agree on a negative correlation of -0.9 or so between their annual or even seasonal mean PMSL values. Fig 6.2B shows the average January PMSL in the Pacific (1961-76) and the position of some of the "key" stations that will be used in the description. The SO fluctuations are usually monitored by an SO index (SOI) which has been defined in many ways; Fig 6.2A indicates that the simplest and best index might be simultaneous values of (Easter Island - Djakarta) PMSL.

Returning to relationships between the SO and South American climate, Fig 6.3 shows superimposed time-series of the level of the great Parana river and a multi-station SO index about a century ago. The correlation is 0.56. However due to better data quality and availability Tahiti and Darwin PMSL have often, if less satisfactorily, been used to provide an SO index. Fig 6.4 shows the seasonal normalised pressure difference between Tahiti and Darwin for 1935 to 1987, updated from Parker (1983). Ropelewski and Jones (1987) have extended the Tahiti pressure series back to 1876, thus enabling the construction of Tahiti minus Darwin indices back to 1882 when the Darwin data began, but there are occasional missing years in the earlier Tahiti data which are a little less reliable than those for 1935 onwards. Fig 6.5 shows a time series of seasonal SSTA for 1856-1987 (relative to the 1951-80 average) calculated for the tropical East Pacific (170°W to S American coast, 20°N to 20°S), an area of about $45 \times 10^6$ $km^2$. The correlation between 3 month seasonal mean tropical East Pacific SSTA

and SO indices between 1935-80 is about -0.65, i.e. warm SSTA is associated with a negative SO index. The tropical East Pacific SSTA variations are (in the main) part of a worldwide fluctuation of SSTA. This is most readily shown in Fig 6.6 which shows the second (correlation matrix) eigenvector (EOF2) of worldwide SSTA calculated for each season and for the available 10° x 10° areas between 1901-80. The time series of the amplitude of EOF2 is shown in Fig 6.7 together with that of the tropical East Pacific SSTA variations; the two time series of EOF2 are strongly correlated (r=0.75). Use of EOF2 does not, however, allow monitoring of systematic changes in the shape of the worldwide SSTA patterns which might occur as "ENSO events" develop, or monitoring of real differences in patterns between events. Despite these limitations, however, a strong, consistent, warming of the Indian Ocean and the northeast Pacific and a similar tendency for simultaneous negative SSTA in the northwest Pacific when the tropical central and eastern Pacific are warm is apparent. Values of the terms of EOF2 of magnitude about 0.6 or over in Fig 6.6 reflect a reasonably consistent relationship with tropical East Pacific SSTA. Fig 6.8 shows spectra of the time-scales of variation of seasonal tropical East and West Pacific SSTA and marine air temperature for 1861-1980 from Folland et al (1985). The East Pacific (basically El Nino) variations occupy the 2.5-16 year time scales. The West Pacific spectrum is distinctly different, being much "whiter".

### 6.1.2 Global temperature variations associated with El Nino

#### 6.1.2.1 SSTA

Fig. 6.9 shows the evolution of Pacific SSTA during El Nino, as presented by van Loon and Shea (1987), based on eight warm events between 1950 and 1979. The early stages in the development of an El Nino during which the warming is confined to S American coastal waters, are not well represented because the resolution used was too coarse. By April of year (0), the S Pacific near the western coast of South America as far south as 35°S shows a distinct warming. A tongue of positive SSTA extends westwards from the South American coast along the Equator, reaching 130°W in May and 170°W by July (see also Newman (1984). The SSTA pattern intensifies, so by

September a large proportion of the Tropical Pacific is warmer than normal and by up to 2°C in the east. In December the warming is at its peak with maximum mean SSTA of 2°C to 3°C. In year (+1) SSTA decline. Both Indian and tropical Atlantic Oceans warm during El Nino, starting in late summer of year (0) (Pan and Oort (1983)). By March of year (+1) much of the Atlantic from 30°N to 30°S is warmer than normal by between 0.2° and 0.5°C (Newman (1984)). The Indian Ocean exhibits maximum mean SSTA of up to 0.6°C at the end of year (0) and the beginning of year (+1) (Cadet (1985)).

By contrast, in April of year (0) an area in the central N Pacific, centred near 30°N, is weakly cool; then the negative SSTA spread northwards and strengthen, giving mean anomalies of -0.8°C in some areas near 40°N between July and October (Fig. 6.9). From November of year (0) to March of year (+1) negative SSTA persist, but are generally weaker. In the northeast extratropical Pacific an area of anomalous warmth spreads northwards near the North American coast in October. This warm area persists until after March of year (+1) (Newman (1984)). From October to December of year (0), the north east Atlantic, polewards of 35°N, is weakly cool with a suggestion of cool SSTA south of 40°S, common to much of the Southern Ocean (Pan and Oort (1983); Newman (1984)). The data are too sparse to be certain, however.

RC used SSTA measured between 1953 and 1974 along 6 ship routes in the area 20°N to 20°S, 70°W to the dateline, to investigate the growth and movement of tropical Pacific SSTA during El Nino. The most common time scales of SSTA fluctuations associated with El Nino (in the area and for the period defined above) were found to be between 36 and 43 months. Cross spectral analysis of SST data at different longitudes indicated that the large scale positive SSTA which initially appear off the coast of Peru about December (eg at Puerto Chicama, see "PC" on Fig 6.2B), spread westward along the Equator, reaching 170°W in 3-6 months. They also noted that equatorial SSTA near the dateline appeared to increase modestly almost simultaneously with the coastal SSTA (cf Fig 6.9(b)). The average westward propagation of SSTA has a speed of 0.5-1.0 m $s^{-1}$. RC also noted a warming of the ocean west of Chile in subtropical latitudes in the year (-1) preceding El Nino.

El Ninos vary considerably in character and in the time intervals between them (eg 3 years between 1969 and 1972, but nine years from 1942-51). This variability may prove crucial to our understanding. For example: the Tropical Pacific west of the dateline was markedly warmer in 1976 than in 1972; in the 1982 event the Tropical E Pacific warmed before the S American coast, which warmed most at the end of the ENSO event, in April-June 1983.The Tropical E Pacific remained warm well into autumn 1983, ie year (+1), and widespread warming of the Indian Ocean exceeded 1.5°C. In 1976, the warming of the Indian Ocean area was weak. The period from 1972 to 1982, during which there were 4 El Ninos (3 of them strong), contrasts with the periods 1942-50 and 1879-1887 when there were none while between 1907 and 1938 El Ninos were few or rather weak (Fig 6.5). Deser and Wallace (1987) document differences in timing and duration of coastal and near-coastal S American SSTA between El Nino events. They note that these SSTA are not very tightly coupled with the SO.

6.1.2.2 Atmospheric Temperature Variations

Pan and Oort (1983) have given a latitude-height cross section of zonal mean temperature differences between three pairs of years having warm and cool East Pacific SST respectively (Fig 6.10) for northern winter. The troposphere as far poleward as 45°N and S warmed by up to 1°C at 400 mb, presumably because of increased moist convection in the tropics. Note also the cooling at middle and high latitudes of about -0.5°C in the Northern Hemisphere, which matches the underlying SST changes fairly well. Yasunari (1987a) obtained similar results.

Pan and Oort also showed that specific humidity rose where air temperature rose and also fell slightly in high latitudes. It is interesting that a tropical forcing (warming) from below has warmed the global troposphere as a whole but that the atmospheric circulation has changed so as to provide a weak cooling in high latitudes. This is rather unexpected, perhaps.

Bradley et al (1987) confirmed the warming associated with ENSO using land surface air temperature data for 0°-30°N.

### 6.1.3 Variations of Atmospheric Circulation

#### 6.1.3.1 General Description

There is now a considerable literature on aspects of the general circulation associated with ENSO or suspected to have a connection with it. The background climatology is described by Horel (1982). RC and Wyrtki (1975) have both shown that ENSO is associated with variations in the Pacific trade wind circulations and the latter author, sea level fluctuations in the Pacific. The tropical easterly jet is weakened and the associated patterns of divergence are weakened and shifted eastward (Chen and van Loon (1987)). Chen (1982) and Horel and Wallace (1981) have indicated links with the Northern Hemisphere mid-latitude circulations; van Loon and Labitzke (1987) describe associations with the stratospheric circulation and Angell (1981) reports associations with ozone over North America and the water vapour content of the low stratosphere; Bacastow and Keeling (1981) note a link with tropospheric $CO_2$ content. ENSO has been proposed as a long range forecasting tool for the Indian monsoon by Shukla and Paolino (1983) and has been used to help make long range forecasts in the USA and New Zealand. However both the Indian monsoon (Wu and Hastenrath (1986); Elliott and Angell (1987)) and atmospheric pressure around New Zealand (Trenberth and Shea (1987)) have more recently been shown to anticipate Southern Oscillation indices. Tropical Pacific SST variations (now defined separately in the Central and East Pacific) have recently been introduced, usefully, as a factor in a statistical long range forecasting technique used in the Synoptic Climatology Branch of the Meteorological Office (Maryon and Storey, 1985). The contrast between El Nino and "La Nina" (cold east tropical Pacific) is discussed by Philander (1985).

### 6.1.3.2 Tropical Atmospheric Variations

The tropical atmosphere is perturbed during ENSO in a complex way as indicated by RC and other authors. In the winter and summer (S Hemisphere) preceeding El Nino, the south east trade winds between 120°W and the dateline are usually abnormally strong giving wind stresses over the tropical S Pacific 50-80% above normal. Relaxation of this stress to below normal levels in the tropical W Pacific in the next summer is followed by the start of El Nino - sometimes the wind stress is reversed, i.e. the winds become westerly. The reason for the weakening is not known, though wind stress is usually less in summer in this region. The triggering mechanism probably comes most often from the Southern Hemisphere but may sometimes arise from the Northern Hemisphere or from within the tropics in association with 40-50 day oscillations (Trenberth and Shea (1987); Lau and Chan (1986)). During year (0) of El Nino, the easterly component of wind stress reaches a minimum but increases once more later in year (0). By contrast, near the equator, between 90°W and about 130°W, the E to SE trades increase in strength to reach a peak during year (0).

The spatial distribution of surface wind anomalies reflects changes in the positions of the Inter-Tropical Convergence Zone (ITCZ) and the South Pacific Convergence Zone (SPCZ) (see Lecture 2). The convergence zones are important in determining the areas of active convection and hence areas of latent heating in the middle and upper troposphere and the rain falling on the "desert" islands of the equatorial Pacific (Lecture 2). Changes in the trade wind circulation also reflect changes in the intensity of the Indonesian Low and Easter Island High, which, as described above, are often used to indicate the phase of the SO.

Figs 6.11(A)-(C) show the anomalous mean tropical Pacific surface winds in an El Nino composite study carried out by RC, shown here for August-October (-1), March-May (0) and December (0) to February (+1). In northern autumn of year (-1) surface wind anomalies are generally small except to the north-east of Australia where anomalous northwesterlies tend

to occur and the SPCZ is displaced to the southwest of its normal position. This displacement probably results from positive SSTA following anomalous northerlies in the subtropical southwest Pacific during the previous 6 months (van Loon and Shea (1985)). The South Pacific High then weakens but the Indonesian Low changes little (van Loon and Shea (1987)). Wind anomalies increase from November (-1) to March (0) with a strong anomalous westerly component (not always giving absolute westerlies) developing south of the Equator and north of 10°S from 170°E to 170°W, reflecting a reduction in strength of the south-east trades. The Indonesian Low fills while the Easter Island High continues to decline. From March to May (0) the same trends in the pressure field continue. Between 110°W and 170°E, the ITCZ is now displaced south of its normal position with anomalous northerlies on its northern side. The anomalous westerly component just south of the Equator now reaches 160°W and there is a strengthening of the south-south east trades in the latitude band 30°S to 10°S from east of Australia to the dateline.

During the remainder of year (0) the anomalous features noted above intensify. In particular the ITCZ continues to be placed south of its climatological position and the SPCZ now becomes located markedly north east of its usual location, reducing the size of the equatorial dry zone (centred near the dateline) between them. During August-October of year (0) the equatorial westerly anomalies are at their strongest exceeding 2 $ms^{-1}$ over much of the Tropical Pacific west of 160°W and an anomalous surface wind convergence is centred near 150°W close to the equator. The Pacific High begins to build again about July followed by a deepening of the Indonesian Low about November. As the El Nino year progresses, the surface wind convergence maximum moves eastwards to near 130°W, the westerly anomaly decreases and the south east trades strengthen between 140-180°W, ie west of the wind convergence.

Pan and Oort (1983) correlated SST in a key area near 2.5°S, 130°W (assumed to represent the entire Tropical E Pacific, a reasonable assumption in view of SSTA analyses presented in Section 6.1.2.1) with global fields of 850 mb and 200 mb wind components and 500 mb vertical velocity.

They found that warm SST (El Nino) is associated with:-

a. Anomalous ascent of air over the Central and much of the Eastern Equatorial Pacific, with anomalous descent of air east of 120°W, over the western Pacific between 110°E and 150°E, and over the subtropics.

b. An increase in the 200 mb subtropical westerlies in both hemispheres near 25° latitude, with anomalous 200 mb easterlies over the Equatorial Pacific, roughly west of the main SSTA maximum.

c. A weakening of surface and 200 mb westerlies near 60°N.

Pan and Oort note that these observations are consistent with Bjerknes' pioneering (1969) explanation of ENSO. Bjerknes (1969) suggested that the normal nearly east-west equatorial Pacific Walker cell, in which air ascends in the convectively active area around Indonesia and descends over the Eastern Pacific near 90°W, is weakened during El Nino. Fig 6.12A shows this cell in more detail (from Kousky et al (1984)). See Lecture 2 for "Walker" cells.

The warm tropical ocean causes the Hadley cell to intensify, leading to stronger 200 mb subtropical jets (Figure 6.12B). In Section 6.1.2.1 it was noted that all three tropical oceans warm during El Ninos, which is consistent with the intensification of subtropical jets at all longitudes. A decrease in the westerlies at 60°N is seen by Pan and Oort as evidence for a stronger than normal Northern Hemisphere Ferrel cell.

Selkirk (1984) has provided an analysis of the 200 mb flow associated with ENSO. He usefully discusses the fluctuations in the light of predictions made by linear models, eg that of Simmons (1982) which shows how the 200 mb and lower tropospheric winds might respond to an anomalous (here a Central or Eastern Pacific) heat source. Chen and van Loon (1987) have contrasted the behaviour of the tropical easterly jet in El Nino and non El-Nino years (see 6.1.3.1 above).

It is essential to note that the above-mentioned composites of El Nino — Southern Oscillation are not completely representative of any individual El Nino — Southern Oscillation event, because each event differs. Some variations in the SSTA signature of El Ninos were described in section 6.1.2.1. Here we document some variations in the atmospheric signature. Figure 6.13, from Trenberth and Shea (1987) shows sequences of Darwin MSL pressure for events since 1939. There are variations in amplitude, in sequence, and in timing, the latter demonstrating the imperfect anchoring of the phase of the SO to the annual cycle. The 1986 event began particularly late, and continued through 1987 with unusual phasing of anomalies relative to the annual cycle. Figure 6.14, from the same paper, shows that both the phase difference and the covariance of MSL pressure between Darwin and several other stations has varied interdecadally. Between 1920 and the late 1930s the SO was relatively inactive, in agreement with Fig. 6.5. Figure 6.15, from Harrison (1987), contrasts the anomalies of surface winds over the Gilbert and Ellice Islands in the central equatorial Pacific during the El Ninos of 1969 and 1972. Harrison also created a composite using winds from these stations: his results were different from RC's in several respects, such as the absence of the persistent off-equatorial meriodional wind anomalies suggested by RC. The zonal components of Harrison's composite wind anomalies were also stronger than RC's and more closely confined to the equator. One reason for the differences was probably that RC used ship data which, in the area around these islands, were rather sparse (Fig. 6.11), giving less reliable results.

### 6.1.3.3 Extra Tropical Relationships with El Nino- Southern Oscillation Events

Many authors have found that the El Nino — Southern Oscillation is associated with changes in extratropical circulations, though teleconnections are less well defined than in the tropics.

Chen (1982) correlated seasonal values of the Tahiti-Darwin Southern Oscillation Index (SOI) with Northern Hemisphere 700 mb geopotential height between 1951 and 1979. He also carried out a composite analysis of the 700 mb data stratified according to the SOI. The composites are shown in Figure 6.16. The winter pattern is quite similar to the 'Pacific North America (PNA)' teleconnection pattern found by Horel and Wallace (1981) (Fig 6.12B) with three centres of response situated at 40°N, 145°W, (high positive correlation), Canada near 125°W (large negative correlation) and near Florida extending towards Spain (high positive correlation). These results were confirmed by Rogers (1984) using MSL pressure and 500 mb geopotential height.Correlations between the 700 mb height field and the SOI of later seasons drop sharply as the lag of SOI behind the 700 mb fields increases. By contrast, correlations reach a maximum when the SOI leads the 700 mb fields by one or two seasons, the response pattern staying broadly similar. However, only in winter with the SOI leading the 700 mb data by one or two seasons is statistical significance at the 95% level unequivocably obtained.

Chen's composite analyses enable non-linearity in the Northern Hemisphere 700 mb atmospheric response to variations in the SOI to be studied. Chen finds that 700 mb height anomalies over the Atlantic are more pronounced with high SOI (low E Pacific SST) (Fig 6.16(A), (B)). However, associations between the Southern Oscillation and the North Atlantic Oscillation are weak (Rogers (1984)).

The Northern Hemisphere extratropical response to ENSO varies between events, as might be expected from a consideration of the variability between events in the tropics described above. Hamilton (1988) found that the PNA pattern in winter was pronounced in EL Nino years when the west tropical Pacific sea surface was anomalously warm, but not when it was anomalously cold. These results confirm the findings of Palmer and Mansfield (1986b) in atmospheric general circulation model studies discussed in Section 6.1.4 below.

In the Southern Hemisphere, the land-sea contrast in summer in 500 mb geopotential height and MSL pressure appears to be modulated by the Southern Oscillation (Mo and White (1985)).

The Southern Oscillation was shown by Barnett (1985) to be part of a global-scale propagating feature in the MSL pressure field. In the light of integrations of an atmospheric general circulation model, it was suggested that the SO resulted from the excitation of a natural dynamical mode of variation within the atmosphere, but that local diabatic forcing by precipitation and remote forcing by Eurasian snow cover, as well as forcing by SST anomalies, were also crucial to the dynamics of the SO. Harrison (1987) found eastward propagation of zonal wind anomalies over the central equatorial Pacific, and so did Cadet (1985) and Yasunari (1987b) over the Indian Ocean but Blazejewski et al (1986) failed to find the eastward propagation of zonal wind anomalies over the Indian Ocean that would have been expected from Barnett's analysis. Trenberth and Shea (1987) suggested that the inferred eastward progression depended on the cyclicity implied by Barnett's analysis in the frequency domain. Fig 6.17, taken from van Loon and Shea (1987), indicates that the major MSL pressure anomalies "arise and move within the core area of the SO on the Southern Hemisphere". Yasunari (1987b), however, considered on the basis of composite fields and lag-correlations that a Eurasian-midlatitude North Pacific interaction may be crucial to ENSO.

### 6.1.3.4 Rainfall Variations

Equatorial rainfall anomalies are an important aspect of El Nino -Southern Oscillation events because of their obvious implications for Pacific 'weather' and because they indicate the position and anomalous intensity of convective activity associated with ENSO. Figure 6.18 shows an annual rainfall series for the central equatorial Pacific; there are very large increases during ENSO events. These local changes may be put in a global context using satellite data as reported by Newman (1984). Figure 6.19 shows the percentage cover of cloud tops with radiative temperatures less than 235K on a 5° x 5° space scale for northern winter and spring

seasons between 1980 and 1983. This index is thought to give a good measure of convective activity. The data are not completely homogeneous in time but are probably spatially reasonably homogeneous. The relative minima in convection over the East Pacific in 1980-82 are the result of the descending branch of the Walker cell. However by March-May 1983, highly anomalous heavy rainfall was reported from the semi-desert Galapagos Islands which turned green as a result; high SSTA persisted and even strengthened again in this region after the earlier peak around December/January 1982-3. NASA (1986) have published an atlas of monthly and seasonal fields of outgoing longwave radiation based on NIMBUS-7 satellite data: the results are in agreement with Fig 6.19.

Ropelewski and Halpert (1987) have analysed the relationships between ENSO and global and regional-scale precipitation patterns, using data from 1875 to 1983. Fig 6.20 illustrates their results for the globe. Relationships are strongest in the Australia-Central Pacific region but are also strong in parts of Southern Africa and South America, and are significant in India. Their paper contains a set of detailed maps like Fig 6.20 for individual regions. Hastenrath et al (1987) obtained slightly grater correlations than implied by Ropelewski and Halpert between the SO and rainfall in the Sahel and some other regions in the Atlantic sector: this may be because Hastenrath et al used regional indices rather than values from individual stations. They also used a shorter period of data (1935-1983). Ropelewski and Halpert note that in some regions, such as the western USA, very different rainfall anomalies accompany different ENSO events. Kiladis and Van Loon (1988) have also presented fields of rainfall anomalies over the Indian and Pacific sectors at different stages of warm - events (El Nino) and cold events (anti - El Nino or La Nina): their results are in accord with those of Ropelewski and Halpert (1987) but are accompanied by corresponding fields of MSL presure and temperature anomalies (consistent with the above accounts) which aid interpretation.

### 6.1.4 AGCM Experiments

Is it physically reasonable that the global atmosphere could respond to El Nino? If so, how? Several experiments using AGCM's have been carried out using El Nino SST forcing; their results broadly support the idea of a widespread tropical response like that observed but give much more variable results in the extratropics. Most of the experiments have concentrated on Northern Hemisphere teleconnections. The first Northern Hemisphere winter AGCM experiment, carried out by Rowntree (1972), indicated, like most subsequent experiments, that a pair of low level low pressure anomalies are forced on either side of the equator near the maximum tropical SSTA (probably nearer the local maximum absolute SST) with upper level anticyclonic anomalies overlying the low pressure centres. Further north a nearly equivalent barotropic response occurs with a low anomaly forced at all levels at about 35-50°N. The general result is to strengthen the Aleutian low. Palmer and Mansfield (1986a, b) carried out extensive experiments on El Nino using the Meteorological Office 11-level AGCM for perpetual winter time conditions. Two of their experiments are discussed below.

#### 6.1.4.1 Experiment 1 "Composite" El Nino SSTA

Palmer and Mansfield (1986a) used a composite of the observed tropical central and eastern Pacific SSTA for northern winter associated with several El Ninos, but doubled in magnitude (Fig 6.21A), with climatological SST elsewhere. They carried out an anomaly experiment with this SSTA and a control experiment without it. Each experiment was continued for 540 model days using "perpetual" January radiation. Anomaly and control experiments both started from real atmospheric data for 28 December 1972, and the model incorporated "envelope" orography whereby mountains are enhanced in height to improve the model's winter climatology.

Fig 6.21B shows the average difference in 200 mb height (anomaly minus control) for these experiments. The "PNA" pattern of Horel and Wallace is evident and was found to be present at all levels. Tropical lows were

overlain by tropical highs as expected. See Lecture 5 for a description of the effects of this upper level anticyclonic "vorticity" forcing. Tests showed that the extratropical Rossby wave-like response was highly statistically significant.

6.1.4.2 Experiment 2 - December 1982 SSTA

The maximum of this real SSTA was to the east of the maximum of the composite SSTA (Fig 6.21C). Palmer and Mansfield (1986b) used two versions of the 11-level AGCM integrated for perpetual winter conditions as before:

(a) Anomaly and control integrations using "envelope" orography, starting from 28 December 1972 atmospheric data;

(b) Anomaly and control integrations for a model with "standard" orography, with the same starting date.

"Envelope" orography has higher mountains than "standard" orography. Both pairs of experiments were integrated for 540 model days.

Figs 6.21D,E show the difference between the anomaly and control experiments for (a) and (b). Neither figure shows a recognisable PNA pattern, and such a pattern was not in fact observed in 1982-83. Both models show a Rossby wave like anomaly response and in both pairs of experiments the response is highly statistically significant - but nevertheless different. In the "standard" orography experiment the anomaly wavelength is longer and the pattern is distorted compared with the "envelope" orography experiment. This is not surprising as the climatological mean flow of the "standard" orography model is much more westerly than that of the "envelope" model in winter, the "envelope" model being thought more realistic.

In a further experiment with weak positive SSTA ( $\simeq 1^{o}C$) in the tropical West Pacific (and envelope orography), Palmer and Mansfield (1986b) obtained a strong PNA pattern, shifted slightly westward relative to that in Fig 6.21B.

We conclude from these experiments that:

(a) The wintertime extratropical response to El Nino may be quite strong but may vary from event to event eg with the longitude or shape of the SSTA or position of the resulting absolute maximum tropical Pacific SST. Palmer and Mansfield found that the responses to different events in their models were too different to be ascribed to the natural atmospheric variability of the models.

(b) The response of an AGCM will depend on its climatology. A realistic local response, as required for long-range forecasting, may demand a realistic representation of the structure of the mean flow.

### 6.1.5 Oceanographic aspects

Gill and Rasmusson (1983) discussed the oceanographic aspects of the 1982-83 El Nino using a model to simulate the response of the mixed layer of the tropical Pacific Ocean to the observed weakening of the trade winds during 1982-3. They assumed a realistic pre-existing gradient of sea surface topography with higher sea-level in the western Pacific than in the eastern Pacific. The east-west difference is typically observed to be about 1 m before El Nino and results from the wind stress imparted by the preceding strong SE trade winds. Fig 6.22A shows the longitude-time plot of the eastward wind stress anomaly used as forcing in the model experiment, Fig 6.22B shows the computed change of surface elevation of the sea from the pre-existing condition where the height was greater in the west, and Fig 6.22C shows the resulting eastward ocean currents. These tended to oscillate in direction on a time scale of about 9 months in their model as a result of the prediction of an eastward moving oceanic equatorial 'Kelvin' wave which was partially reflected from the S American coast in the form of an equatorially trapped Rossby wave. Such Kelvin waves have been observed by satellite-based altimeters (Miller et al (1988)). The model of Gill and Rasmusson produced a good simulation of the observed change of sea-level topography and ocean currents during the 1982-3 ENSO. Their model results were also consistent with the observation

in 1982-83 of eastward propagation of the main warming of SST towards the central Pacific with even later warming near S America (Fig 6.23D). However, this behaviour, though correct for 1982-3, is not always typical (section 6.1.2.1). Graham and White (1988) have collated evidence that ENSO is a natural oscillator involving not only an oceanic equatorial Kelvin wave but also a simultaneous oceanic off-equatorial Rossby wave which is reflected from the western boundary into the equatorial zone as a Kelvin wave of opposite phase from the one further east.

Cane et al (1986) have used a simplified model of the coupled ocean-atmosphere system to make successful hindcasts of El Nino (Fig 6.23). Their model included thermocline depth or heat content of the upper ocean, currents, SST, and surface winds, over the tropical Pacific. The success of hindcasts made starting up to 2 years before El Nino events was taken as evidence that the sub-surface ocean has an active role in the generation of El Nino.

Sperber et al (1987) have succeeded in simulating the SO in a global model of the coupled atmosphere and upper ocean.

Taken as a whole, the model simulations of ENSO clearly show the need for fully detailed coupled ocean-atmosphere models. Development of these is proceeding apace.

### 6.1.6 Conclusion

The ENSO event represents the most important non-seasonal, if irregularly recurring, event in the climate system on time scales between the annual cycle and the ice ages that has yet been properly identified. The factors that initiate the El Nino/ENSO sequence remain elusive. Some of the physical processes that occur in the ocean and the atmosphere during ENSO have nevertheless been isolated.

## 6.2 THE QUASI-BIENNIAL OSCILLATION

### 6.2.1 Introduction

A brief description is given of this curious lower-stratospheric phenomenon which was discovered almost simultaneously by Ebdon (1960) and Reed (1960). The QBO is the only known example in the climate system of a quasi-periodic process of reasonably regular behaviour whose time scale lies between the annual and ice-age time scales. The next most regular process is the ENSO phenomenon discussed in Part I. Although the links between the QBO and surface climate are tenuous, we justify its inclusion here:-

(a) To provide a background to the discussion of volcanic dust and climate in Lecture 3. The QBO affects our ability to detect and interpret the effects of volcanic dust on stratospheric temperature and thus to unravel the physical properties of volcanic dust.

(b) Because of the possibility of links with climatic phenomena such as ENSO and fluctuations of the Indian northern summer monsoon (Quiroz (1983); Bhalme et al (1987)).

### 6.2.2 Description

The QBO shows up most prominently as a quasi-biennial oscillation of zonal wind and temperature in the tropical lower stratosphere within 15° of the equator. Fig 6.24A shows the monthly mean 30 mb zonal winds above Canton Island (Central Pacific) for 1954-1967, Gan (Central Indian Ocean) for 1967-75, and Singapore for 1976-87. Corresponding 50 mb winds from 1953 are shown in Fig 6.24B. The associated temperature changes over Singapore between 50 mb, and 150 mb where they disappear, for part of the period are shown in Fig 6.25. Temperatures are higher by several °C in the westerly phase. It is possible to form composite time series such as Fig 6.24 from such widely-separated tropical stations because the QBO occurs on

a global scale in the tropics with very little phase-lag between different longitudes at a given elevation. The period of the QBO is not constant: it varies from less than 2 years to about 3 years, and averages 2 years and 3 months. The period does not appear to be related to ENSO or (on the basis of Agung and El Chichon) to volcanic eruptions (Angell (1986); Naujokat (1986)). Periods close to either 2 or 3 years tend to be favoured, and there are also favoured seasons for reversal of the 50 mb or 30 mb wind directions (Dunkerton and Delisi (1985)). A downwards phase propagation of the oscillation occurs; for example, changes in the 50 mb wind vector lag several months behind similar changes in the 30 mb wind vector (Fig 6.26). The maximum amplitude is near 20 mb (Naujokat (1986)). Easterlies are generally stronger than westerlies (Fig 6.24), and are of longer duration than westerlies at 10-30 mb but of shorter duration than westerlies at 40-70 mb (Naujokat (1986)), ie the westerly zones propagate downwards faster.

The discovery of the tropical stratospheric QBO has been followed by widespread reports of quasi-biennial behaviour in local tropospheric climate and circulation parameters. Parthasarathy and Mooley (1978) found a quasi-biennial oscillation in Indian northern summer monsoon rainfall, but this was not strong and regular enough to be used for forecasting. Ebdon (1975) documented anomalies in the Northern hemisphere mid-latitude mean sea level pressure and 500 mb geopotential patterns, and in zonal winds aloft, that varied according to the phase of the tropical 30 mb QBO. Figure 6.27 illustrates the mean sea level pressure anomaly in the extratropical Northern Hemisphere for Julys with a westerly tropical QBO wind mode at 30 mb. The anticyclonic anomaly near the British Isles was found to be statistically significant at about the 5% level. In addition, not only Ebdon (1975) but also Angell and Korshover (1977) observed that the circumpolar upper-tropospheric vortex was smaller during the westerly phase of the tropical 50 mb QBO, particularly in winter, with an associated increase of tropospheric temperature of several tenths °C in mid-latitudes. Consequent possible associations with, for example, summer temperature and sunshine in the United Kingdom, were noted by Ebdon and also by Folland (1977). Holton and Tan (1980) (Fig 6.28) have demonstrated that there may be a 50 mb and a 1000 mb quasi-biennial oscillation in the winter

geopotential and temperature of the northern polar regions. The two atmospheric levels oscillate in phase but the amplitude is weaker at 1000 mb. The oscillation appears to be in antiphase with the tropical 50 mb QBO. Van Loon and Labitzke (1987) confirmed Holton and Tan's results at 50 mb by comparing winters at opposite phases of the tropical QBO but excluding El Nino or anti-El Nino years because, as they demonstrated, the ENSO also affects the stratospheric circulation. It must, however, be emphasised that observations of QBO outside the tropical stratosphere have been associated only statistically with the tropical stratospheric QBO at this stage. Physical associations have not been established.

### 6.2.3 Theories

The physical causes of the tropical stratospheric QBO were investigated in a theoretical paper by Holton and Lindzen (1972). The essence of their hypothesis was that transfer of momentum from upward-propagating equatorial Kelvin and Rossby-gravity waves in zones of vertical shear of zonal wind could explain the observed downward-propagating shear zones (Fig 6.29). The waves originated in the troposphere and lost their momentum in the stratosphere because they were absorbed by radiative damping. Westerly momentum was imparted by the decaying Kelvin waves to the stratosphere in the shear zone beneath the downward propagating westerly phase of the QBO, and the Rossby-gravity waves performed a similar function in regard to the easterly phase. Their hypothesis has subsequently been modified by a variety of workers. The processes by which the waves are absorbed may be mechanical (ie turbulent) as well as radiative (Plumb (1984)). Dunkerton (1985) as well as Plumb (1984) and Hamilton (1984) discuss the influence of the circulation in the vertical-meridional plane; and the effects of absorption of solar radiation by ozone may also be important (Dunkerton (1985), as the concentration of ozone is modulated by the QBO. The vertical meridional circulation appears to be responsible for the fact that the downward propagation of westerly zones is faster than that of easterly zones. The one-dimensional model of Tanaka and Yoshizawa (1987) fails to reproduce this feature, whereas the two-dimensional model of Takahashi (1987) succeeds in obtaining this and other observed details of the morphology of the QBO, such as the

appearance, at a given level, of westerlies, but not easterlies, on the equator before they appear at other latitudes (Fig. 6.30). The QBO has not yet been reproduced in atmospheric general circulation models because their vertical resolution is too coarse and their damping coefficients are probably too great (Plumb (1984)).

The mechanisms by which the tropical lower stratospheric quasi-biennial oscillation might affect the rest of the atmosphere are completely uncertain. It is just possible that the associated temperature changes near the tropical tropopause (Fig 6.25) may affect the strength of tropical convection where it is most powerful, eg over the tropical West Pacific, and thereby influence the Hadley or Walker cells and subsequently the rest of the circulation. It is known that tropospheric air almost certainly regularly enters the stratosphere in this region (Newell and Gould-Stewart (1981)). Recent work also indicates that the Indian northern summer monsoon rainfall is modulated by the QBO (Bhalme et al (1987)).

### 6.2.4 Angular momentum considerations

In the Northern Hemisphere summer the difference in the contribution to the axial angular momentum of the Northern Hemisphere atmosphere by a maximum westerly phase of QBO compared with a maximum easterly phase may sometimes be 5%-10% of the total Northern Hemisphere axial angular momentum, allowing for the phase lags of the QBO with height. The development of a westerly phase of the QBO represents an increase in the axial momentum of the atmosphere where it is already by definition a maximum. At all phases, small compensating changes in atmospheric circulation that preserve axial angular momentum should occur somewhere else (in either hemisphere). Note that this momentum cannot be transmitted to the earth's rotation in a direct way as the stratospheric oscillation occurs well above the level of any mountains, though the transfer could occur indirectly through a tropospheric circulation change.

## 6.3 THE 30- TO 60-DAY VARIATIONS

### 6.3.1 Discovery

Madden and Julian (1971) appear to have been the first to detect an oscillation of 40- to 50-day time-scale in tropospheric zonal wind and temperature and surface pressure in the tropical Pacific. They found that the upper- and lower-tropospheric zonal winds were in antiphase and that surface pressure was in phase with lower-tropospheric westerlies and in antiphase with temperatures throughout the troposphere. Madden and Julian speculated that the oscillation was a large circulation cell oriented in zonal planes and centred in the mid-Pacific. They could not detect the oscillation further afield at Singapore or in the Panama Canal Zone. Further analysis (Madden and Julian (1972)) suggested that the oscillation resulted from eastward-moving wavenumber 1 or 2 circulation cells oriented in the equatorial plane, originating in the Indian Ocean and propagating to the eastern Pacific.

In the following account, the broad-band nature of the variations is shown by the range of time scales quoted, e.g. 30 to 50 days, 30 to 60 days etc. The variations have sometimes been called the "seven-week fluctuations".

### 6.3.2 Detailed description

Using 200 mb, 850 mb and surface pressure data for December 1978 to November 1979 obtained during the First GARP Experiment, (FGGE) (which included the Monsoon Experiment (MONEX) in the Indian Ocean-South Asia region), Krishnamurti et al (1985) identified a planetary-scale divergence and pressure wave of 30- to 50-day time-scale traversing the globe eastward at about 8° longitude per day (Fig 6.31). The divergent circulations were thermally direct over the Asian monsoon region and the western tropical Pacific, but were thermally indirect and became weaker over the eastern tropical Pacific and the tropical Atlantic. There was northward propagation in the Indian monsoon region in northern summer (Fig 6.32),

modulating the intensity of the monsson and triggering its onset and withdrawal via interactions with a 10- to 20-day westward-propagating pressure perturbation.

Graves and Stanford (1987) found 40- to 50-day atmospheric oscillations over the southern Pacific. These differed from those found by Madden and Julian in that the zonal wind fluctuations were in phase throughout the troposphere. The temperature fluctuations at 100 mb, partly monitored with a satellite-based microwave sounding unit, were found to be out of phase with those at 250 mb to 500 mb. The oscillations were enhanced during the 1982-3 El Nino.

Research into these intraseasonal variations was intensified when fields of outgoing longwave radiation (OLR) data became available from satellites. These data indicate the location of deep convection: when the clouds are thick and their tops high and cold, outgoing longwave radiation is reduced. Lau and Chan (1985, 1986) have performed extensive analyses for northern winter and northern summer respectively. In northern winter, the dominant pattern of tropical convection was found to be an east-west oriented dipole propagating eastward along the equator from the Indian Ocean but stalling and intensifying on reaching the maritime continent and the equatorial central Pacific. There was also southeastward propagation into the monsoonal region of Australasia, and evidence of interactions with the atmosphere over Asia and the subtropical North Pacific. It was suggested that 40- to 50-day wave activity may have triggered the 1982-3 El Nino — Southern Oscillation event. In northern summer, there was still eastward propagation along the equator from the Indian Ocean to the western Pacific, but there was also northward propagation from the Indian Ocean towards the Indian subcontinent (in agreement with Krishnamurti et al (1985)) and northwestward propagation from the western Pacific towards southern China (Fig 6.33). Again the oscillation was found to modulate the Indian monsoon and to be phase-locked to the monsoon onset over India and to the Mei-yu (plum) rains over southern China. It was suggested that the northward propagation arises through interaction between the eastward-propagating equatorial modes and the monsoon cirulations.

Murakami et al (1986) obtained results consistent with those of Lau and Chan but observed that occasionally the 30- to 60-day perturbations exhibited irregular propagation. On such occasions, the teleconnection patterns were weak. A subsequent study (Shrestha and Murakami (1988)), confined to occasions with systematic eastward propagation, found that, in northern summer, surges of southerlies at 850 mb near northern Madagascar on the 30- to 60-day time-scale were followed by intensification of the monsoonal westerlies near south India and eventually by enhancement of convective activity over the Asian monsoon region. Similar surges off western Australia tended to activate convection over the western equatorial Pacific. Transient ( < 30 days) disturbances over India and over the subtropical southern Indian Ocean were found to be amplitude-modulated on a 30- to 60-day time-scale, but this was not the case near the equator. Thus transient disturbances over the subtropics could also be an energy source for the 30- to 60-day fluctuations there. Sumathipala and Murakami (1988) found analogous characteristics over the Australia - Indonesia - western Pacific sector in northern winter: in this case surges in the low-level northeasterlies from the Pacific, rather than in the low-level northerlies from Siberia, played the significant role in Australian monsoon activity.

Fig 6.34 is a schematic depiction of the structure of the 40- to 50-day oscillation taken from the seasonal analysis by Madden (1986) of the 40- to 50-day oscillation in the tropics. Madden found that the oscillation was strongest during northern winter and weakest with less regular eastward propagation during northern summer, and confirmed that it was stronger in the Indian Ocean and western Pacific than elsewhere. The upper- and lower-tropospheric zonal winds were most coherently out of phase at near-equatorial stations in the summer hemisphere, suggesting that the oscillation gains its energy from the deep convection associated with the seasonal migration of the intertropical convergence zone. At 150 mb over the Indian Ocean and western Pacific, the zonal and meridional winds were coherent and out of phase in northern winter but in phase in northern summer, consistent with the anticyclone marked in Fig 6.34 and with the hypothesis of fluctuations associated with stronger and weaker convection in the intertropical convergence zone. The greater regularity of the

eastward progression in northern winter, when the convective heating is nearer the equator, was taken as an indication, supported by numerical modelling studies, that the oscillation is at least partly a Kelvin-wave response to this heating.

Madden (1986) also includes a discussion of unexplained features of the 40-to 50-day oscillation, including the absence of Rossby waves, which numerical model studies indicate should propagate westward from areas of equatorial convection, and a review of progress in modelling the oscillation.

### 6.3.3 Conclusion

The importance of the 30- to 60-day variations to the climate of at least the tropics cannot be over-stressed. They appear, from the foregoing discussion, to be linked to both El Nino-Southern Oscillation and to the Asian northern summer monsoon. The Quasi-Biennial Oscillation in the equatorial lower stratosphere is probably driven by transfer of momentum from Kelvin and Rossby-gravity waves propagating upwards from the troposphere (see Section 6.2), and waves of this type seem to be implicated in the 30- to 60-day oscillations. Thus the discovery by Bhalme et at (1987) of links between the Quasi-Biennial Oscillation and the fluctuations of the Indian northern summer monsoon rainfall should, perhaps, come as no surprise.

## REFERENCES TO ADVANCED LECTURE 6

### 6.1 EL NINO/SOUTHERN OSCILLATION


ANGELL, J K (1981) Comparison of variations in atmospheric quantities with sea surface temperature variations in the equatorial eastern Pacific. Mon Weath Rev, 109, 230-243.

BACASTOW, R B and KEELING, C D (1981) Atmospheric $CO_2$ and the Southern Oscillation; effects associated with recent El Nino events. Proc WMO/ICSU/UNEP Conf on Analysis and Interpretation of Atmospheric $CO_2$ data, pp 109-112. WCP-14, Geneva.

BARNETT, T P (1985) Variations in near-global sea level pressure. J Atm. Sci., 42, 478-501.

BERLAGE, H P (1966) The Southern Oscillation and world weather. Mededel. Verhandel. 88, Kon Ned Met Inst, 152 pp.

BERLAGE, H P and DE BOER, H J (1959) On the extension of the Southern Oscillation throughout the world during the period July 1 1949-July 1 1957. Geofis Pure Appl, 44, 287-295.

BJERKNES, J (1969) Atmospheric teleconnections from the equatorial Pacific. Mon. Weath. Rev., 97, 163-172.

BLAZEJEWSKI, H, CADET, D L and MARSAL, O (1986) Low-frequency sea surface temperature and wind variations over the Indian and Pacific Oceans. J Geophys. Res., 91, C4, 5129-5132.

BRADLEY, R S, DIAZ, H F, KILADIS, G N and EISCHEID, J K (1987) ENSO signal in continental temperature and precipitation records. Nature, 327, 497-501.

CADET, D L (1985) The Southern Oscillation over the Indian Ocean. J Climatology, 5, 189-212.

CANE, M A, ZEBIAK, S E and DOLAN, S C (1986) Experimental forecasts of El Nino. Nature, 321, 827-832.

CHEN, T-C and van LOON, H (1987) Interannual variations of the tropical easterly jet. Mon. Weath. Rev., 115, 1739-1759.

CHEN, W Y (1982) Fluctuations in northern hemisphere 700 mb height field associated with the Southern Oscillation. Mon Weath Rev, 110, 808-823.

DESER, C and WALLACE, J M (1987) El Nino events and their relation to the Southern Oscillation: 1925-1986. J. Geophys. Res., 92, C13, 14189-14196

ELLIOTT, W P and ANGELL, J K (1987) The relation between Indian Monsoon rainfall, the Southern Oscillation, and hemispheric air and sea temperature: 1884-1984. J. Clim. Appl. Met., 26, 943-948.

FOLLAND, C K, PARKER, D E and NEWMAN, M R (1985) Worldwide marine temperature variations on the season-to-century time scale. Proc 9th Climate Diagnostics Conf, Corvallis, Oregon, 22-26 Oct 1984, pp 70-85. NOAA.

GILL, A E and RASMUSSON, E M (1983) The 1982-83 climate anomaly in the equatorial Pacific. Nature, 306, 229-234.

GODBOLE, R V and SHUKLA, J (1981) Global analysis of January and July sea level pressure. NASA Tech Mem 82097, Goddard Space Flight Center, Greenbelt, Maryland 20771.

GRAHAM, N E and WHITE, W B (1988) The El Nino cycle; a natural oscillator of the Pacific Ocean-atmosphere system. Science, 240, 1293-1302.

HAMILTON, K (1988) A detailed examination of the extratropical response to tropical El Nino/Southern Oscillation events. J. Climatology, 8, 67-86.

HARRISON, D E (1987) Monthly mean island surface winds in the central tropical Pacific and El Nino events. Mon. Weath. Rev., 115, 3133-3145.

HASTENRATH, S., de CASTRO, L C and ACEITUNO, P (1987) The Southern Oscillation in the tropical Atlantic sector. Beitr. Phys. Atm., 60, 447-463.

HILDEBRANDSSON, H H., (1897) Quelques recherches sur les centres d'action de l'atmosphere. K. Svenska Vetens.-Akad. Handl., 29, 33 pp.

HOREL, J D (1982) On the annual cycle of the tropical Pacific atmosphere and ocean. Mon Weath Rev, 110, 1863-1878.

HOREL, J D and WALLACE, J M (1981) Planetary scale atmospheric phenomena associated with the Southern Oscillation. Mon Weath Rev, 109, 813-829.

KILADIS, G N and VAN LOON, H (1988) The Southern Oscillation. Part VII: Meteorological anomalies over the Indian and Pacific sectors associated with the extremes of the oscillation. Mon. Weath. Rev., 116, 120-136.

KOUSKY, V E, KAGANO, M T and CAVALCANTI, I F A (1984) A review of the Southern Oscillation: oceanic-atmospheric circulation changes and related rainfall anomalies. Tellus, 36A, pp 490-504.

LAU, K-M and CHAN, P H (1986) Aspects of the 40-50 day oscillation during the northern summer as inferred from outgoing longwave radiation. Mon. Weath. Rev., 114, 1354-1367.

LOCKYER, N., and LOCKYER, W J S (1902a) On some phenomena which suggest a short period of solar and meteorological changes. Proc. Roy. Soc. London, 70, 500.

LOCKYER, N and LOCKYER W J S (1902b) On the similarity of the short-period pressure variation over large areas. Proc. Roy. Soc. London, 71, 134-135.

LOCKYER, N and LOCKYER W J S (1904) The behaviour of the short-period atmospheric pressure variation over the earth's surface. Proc. Roy. Soc. London, 73, 457-470

LOCKYER, W J S (1906) Barometric variations of long duration over large areas. Proc. Roy. Soc. London, A78, 43-60.

MARYON, R H and STOREY, A M (1985) A multivariate statistical model for forecasting anomalies of half-monthly mean surface pressure. J Climatology, 5, 561-578.

MILLER, L, CHENEY, R E and DOUGLAS, B C (1988) GEOSAT altimeter observations of Kelvin waves and the 1986-87 El Nino. Science, 239, 52-54.

MO, K C and WHITE, G H (1985) Teleconnections in the Southern Hemisphere. Mon. Weath. Rev., 113, 22-37.

MOSSMAN, R C (1924) Indian monsoon rainfall in relation to South American weather, 1875-1914. Mem Indian Met Dept, 23, 157-242.

NATIONAL AERONAUTICS AND SPACE ADMINISTRATION (NASA) (1986) El Nino and outgoing longwave radiation: an atlas of NIMBUS-7 Earth Radiation Budget observations. NASA Ref. Publ. 1163, 92pp.

NEWMAN, M R (1984) Observational aspects of the El Nino and the atmospheric response. Met O 13 Branch Memo 148.

PALMER, T N and MANSFIELD, D A (1986a) A study of wintertime circulation anomalies during past El Nino events using a high resolution general circulation model. I: Influence of model climatology. Quart. J. Roy. Met. Soc., 112, 613-638.

PALMER, T N and MANSFIELD, D A (1986b) A study of wintertime circulation anomalies during past El Nino events using a high resolution general circulation model. II: Variability of the seasonal mean response. Quart. J. Roy. Met. Soc., 112, 639-660.

PAN, Y H and OORT, A H (1983) Global climate variations connected with sea surface temperature anomalies in the eastern equatorial Pacific Ocean for the 1958-73 period. Mon Weath Rev, 111, 1244-1258.

PARKER, D E (1983) Documentation of a Southern Oscillation index. Met Mag, 112, 184-188.

PHILANDER, S G H (1985) El Nino and La Nina. J Atm Sci, 42, 2652-2662.

QUIROZ, R S (1983) The climate of the "El Nino" winter of 1982-83 - a season of extraordinary climatic anomalies. Mon Weath Rev, 11, 1685-1706.

RASMUSSON, E M and CARPENTER, T H (1982) Variations in tropical sea surface temperature and surface wind fields associated with the Southern Oscillation/El Nino. Mon Weath Rev, 110, 354-384.

ROGERS, J C (1984) The association between the North Atlantic Oscillation and the Southern Oscillation in the Northern Hemisphere. Mon. Weath. Rev., 112, 1999-2015.

ROPELEWSKI, C F and HALPERT, M S (1987) Global and regional scale precipitation patterns associated with the El Nino/Southern Oscillation. Mon. Weath. Rev., 115, 1606-1626.

ROPELEWSKI, C F and JONES, P D (1987) An extension of the Tahiti-Darwin Southern Oscillation Index. Mon. Weath. Rev., 115, 2161-2165.

ROWNTREE, P R (1972) The influence of tropical east Pacific Ocean temperatures on the atmosphere. Quart J Roy Met Soc, 98, 290-321.

SELKIRK, R (1984) Seasonally stratified correlations of the 200 mb tropical wind field to the Southern Oscillation. J Climatology, 4, 365-382.

SHUKLA, J and PAOLINO, D A (1983) The Southern Oscillation and long-range forecasting of the summer monsoon rainfall over India. Mon Weath Rev, 111, 1830-1837.

SIMMONS, A J (1982) The forcing of stationary wave motion by tropical diabatic heating. Quart J Roy Met Soc, 108, 503-534.

SPERBER, K R, HAMEED, S, GATES, W L and POTTER, G L (1987) Southern Oscillation simulated in a global climate model. Nature, 329, 140-142.

TRENBERTH, K E and SHEA, D J (1987) On the evolution of the Southern Oscillation. Mon. Weath. Rev., 115, 3078-3096.

VAN LOON, H, and LABITZKE, K (1987) The Southern Oscillation Part V. The anomalies in the lower stratosphere of the Northern Hemisphere in winter and a comparison with the Quasi-Biennial Oscillation. Mon. Weath. Rev., 115, 357-369.

VAN LOON, H and SHEA, D J (1985) The Southern Oscillation Part IV. The precursors south of 15°S to the extremes of the Oscillation. Mon. Weath. Rev., 113, 2063-2074.

VAN LOON, H and SHEA, D J (1987) The Southern Oscillation Part VI. Anomalies of sea level pressure on the Southern Hemisphere and of Pacific sea surface temperature during the development of a warm event. Mon. Weath. Rev., 115, 370-379.

WALKER, G T (1923) Correlation in seasonal variations of weather. VIII: A preliminary study of world weather. Mem. Indian Met. Dept., 24, 75-131.

WALKER, G T (1924) Correlation in seasonal variations of weather. IX: A further study of world weather. Mem. Indian Met. Dept., 24, 275-332.

WALKER, G T (1928) World Weather III. Mem. Roy. Met. Soc., 2, 97-106.

WALKER, G T and BLISS, E W (1930) World Weather IV. Mem. Roy. Met. Soc., 3, 81-95.

WALKER, G T and BLISS, E W (1932) World Weather V. Mem. Roy. Met. Soc., 4, 53-84.

WALKER, G T and BLISS, E W (1937) World Weather VI. Mem. Roy. Met. Soc., 4, 119-139.

WU, M-C and HASTENRATH, S (1986) On the interannual variability of the Indian Monsoon and the Southern Oscillation. Arch. Met. Geoph. Biocl. Ser.B 36, 239-261.

WYRTKI, K (1975) El Nino - the dynamic response of the equatorial Pacific Ocean to atmospheric forcing. J Phys Ocean, 5, 572-584.

YASUNARI, T (1987a) Global structure of the El Nino/Southern Oscillation. Part I El Nino composites. J. Met. Soc. Japan, 65, 67-80.

YASUNARI, T (1987b) Global structure of the El Nino/Southern Oscillation. Part II. Time evolution. J. Met. Soc. Japan 65, 81-102.

## 6.2 QUASI-BIENNIAL OSCILLATION

ANGELL, J K (1986) On the variation in period and amplitude of the Quasi-Biennial Oscillation in the equatorial stratosphere 1951-85. Mon Weath Rev, 114, 2272-2278.

ANGELL, J K and KORSHOVER, J (1977) Variation in size and location of the 300 mb north circumpolar vortex between 1963 and 1975. Mon Weath Rev, 105, 19-25.

BHALME, H N, RAHALKAR, S S and SIKDER, A B (1987) Tropical quasi-biennial oscillation of the 10-mb wind and Indian monsoon rainfall — implications for forecasting. J Climatology, 7, 345-353.

DUNKERTON, T J (1985) A two-dimensional model of the Quasi-Biennial Oscillation. J Atm Sci, 42, 1151-1160.

DUNKERTON, T J and DELISI, D P (1985) Climatology of the equatorial lower stratosphere. J Atm Sci, 42, 376-396.

EBDON, R A (1960) Notes on the wind flow at 50 mb in tropical and sub-tropical regions in January 1957 and January 1958. Quart J Roy Met Soc, 86, 540-542.

EBDON, R A (1975) The quasi-biennial oscillation and its association with tropospheric circulation patterns. Met Mag, 104, 282-297.

FOLLAND, C K (1977) Recent work on some quasi-cyclic fluctuations of meteorological parameters affecting British climate. Weather, 32, 336-342.

HAMILTON, K (1984) Mean wind evolution through the quasi-biennial cycle in the tropical lower stratosphere. J. Atm. Sci., 41, 2113-2125.

HOLTON, J R AND LINDZEN, R S (1972) An updated theory for the quasi-biennial cycle of the tropical stratosphere. J Atm Sci, 29, 1076-1080.

HOLTON, J R AND TAN, H-C (1980) The influence of the equatorial quasi-biennial oscillation on the global circulation at 50 mb. J Atm Sci, 37, 2200-2208.

NAUJOKAT, B (1986) An update of the observed Quasi-Biennial Oscillation of the stratospheric winds over the tropics. J Atm Sci, 43, 1873-1877.

NEWELL, R E AND GOULD-STEWART, S (1981) A stratospheric fountain? J Atm Sci, 38, 2789-2796.

PARTHASARATHY, B AND MOOLEY, D A (1978) Some features of a long homogeneous series of Indian summer monsoon rainfall. Mon Weath Rev, 106, 771-781.

PLUMB, R A (1984) The Quasi-Biennial Oscillation. In "Dynamics of the Middle Atmosphere", Eds. J R Holton and T Matsuno, Adv. Earth Planet. Sci., Tokyo (Terra) and Dordrecht (D Reidel), pp 217-251.

QUIROZ, R S (1983) Relationships among the stratosphere and tropospheric zonal flows and the Southern Oscillation. Mon Weath Rev, 111, 143-154.

REED, R J (1960) The circulation of the stratosphere. Paper presented at the 40th Annual meeting of the American Met Soc, Boston, Mass.

TAKAHASHI, M (1987) A 2-dimensional numerical model of the Quasi-Biennial Oscillation: Part I. J Met Soc Japan, 65, 523-536.

TANAKA, H and YOSHIZAWA, N (1987) A slowly varying model of the Quasi-Biennial Oscillation involving effects of transience, self-acceleration and saturation of equatorial waves. J Atm Sci, 44, 1427-1436.

VAN LOON, H and LABITZKE, K (1987) The Southern Oscillation. Part V: The anomalies in the lower stratosphere of the Northern Hemisphere in winter and a comparison with the Quasi-Biennial Oscillation. Mon Weath Rev, 115, 357-369.

## 6.3 30- TO 60-DAY VARIATIONS

BHALME, H N, RAHALKAR, S S and SIKDER, A B (1987) Tropical quasi-biennial oscillation of the 10-mb wind and Indian monsoon rainfall — implications for forecasting. J Climatology, 7, 345-353.

GRAVES, C E and STANFORD, J L (1987) Low-frequency atmospheric oscillations over the southeastern Pacific. J Atm Sci, 44, 260-264.

KRISHNAMURTI, T N, JAYAKUMAR, P K, SHENG, J, SURGI, N and KUMAR, A (1985) Divergent circulations on the 30 to 50 day time scale. J Atm Sci, 42, 364-375.

LAU, K-M and CHAN, P H (1985) Aspects of the 40-50 day oscillation during the northern winter as inferred from outgoing longwave radiation. Mon Weath Rev, 113, 1889-1909.

LAU, K-M and CHAN, P H (1986) Aspects of the 40-50 day oscillation during the northern summer as inferred from outgoing longwave radiation. Mon Weath Rev, 114, 1354-1367.

MADDEN, R A (1986) Seasonal variations of the 40-50 day oscillation in the tropics. J Atm Sci, 43, 3138-3158.

MADDEN, R A and JULIAN, P R (1971) Detection of a 40-50 day oscillation in the zonal wind in the tropical Pacific. J Atm Sci, 28, 702-708.

MADDEN, R A and JULIAN, P R (1972) Description of global-scale circulation cells in the tropics with a 40-50 day period. J Atm Sci, 29, 1109-1123.

MURAKAMI, T, CHEN, L-X, XIE, A and SHRESTHA, M L (1986) Eastward propagation of 30-60 day perturbations as revealed from outgoing longwave radiation data. J Atm Sci, 43, 961-971.

SHRESTHA, M L and MURAKAMI, T (1988) Intraseasonal fluctuations in low-level meridional winds over the Indian Ocean and monsoonal convection over South Asia. Tellus, 40A, 120-132.

SUMATHIPALA, W L and MURAKAMI, T (1988) Intraseasonal fluctuations in low-level meridional winds over the South China Sea and the western Pacific and monsoonal convection over Indonesia and northern Australia. Tellus, 40A, 205-219.

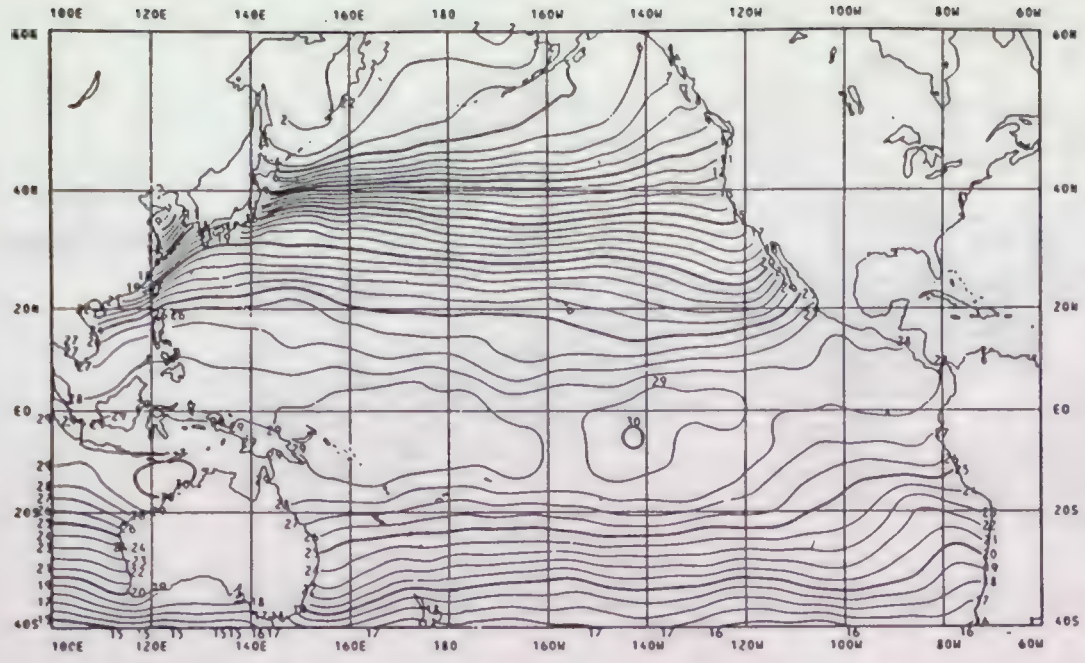


Sea surface temperature over the Pacific Ocean for winter 1982–83.

Figure 6.1A. From Quiroz (1983).

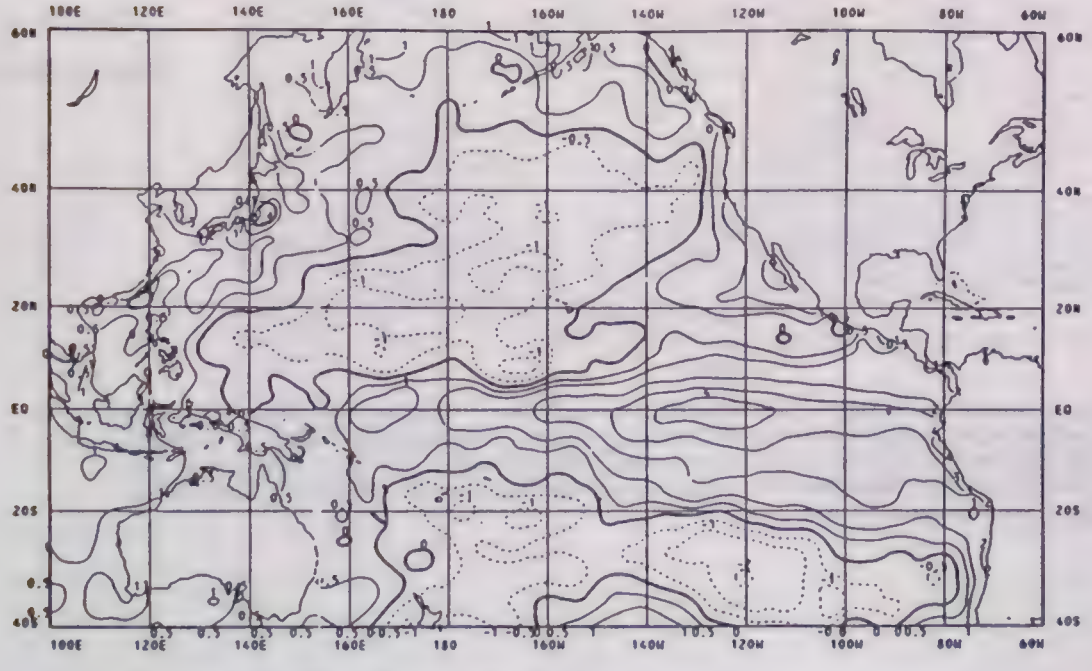


Sea surface temperature (°C) for winter 1982–83 over the Pacific Ocean. Dashed lines portray negative anomalies, thin solid lines indicate positive anomalies, and the heavy solid line is the zero line. Anomalous isotherms are at 1°C intervals except for 0.5°C between +1 and −1°C.

Figure 6.1B. From Quiroz (1983).

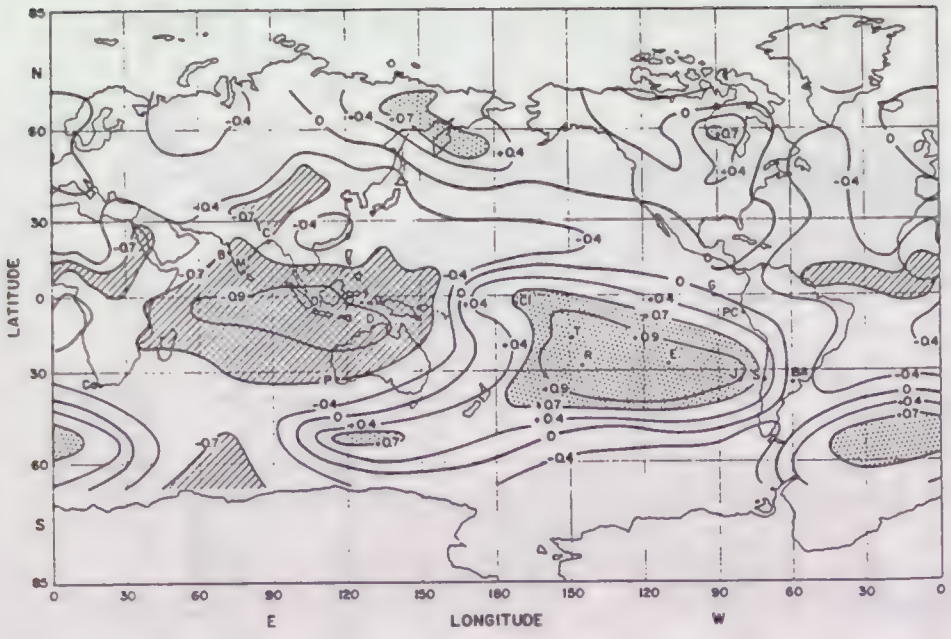


Figure 6.2A.
From Kousky et al (1984)

Isolines of correlation coefficients of sea level pressure anomalies using Easter Island (E) as the reference station. Adapted from Berlage and de Boer (1959).

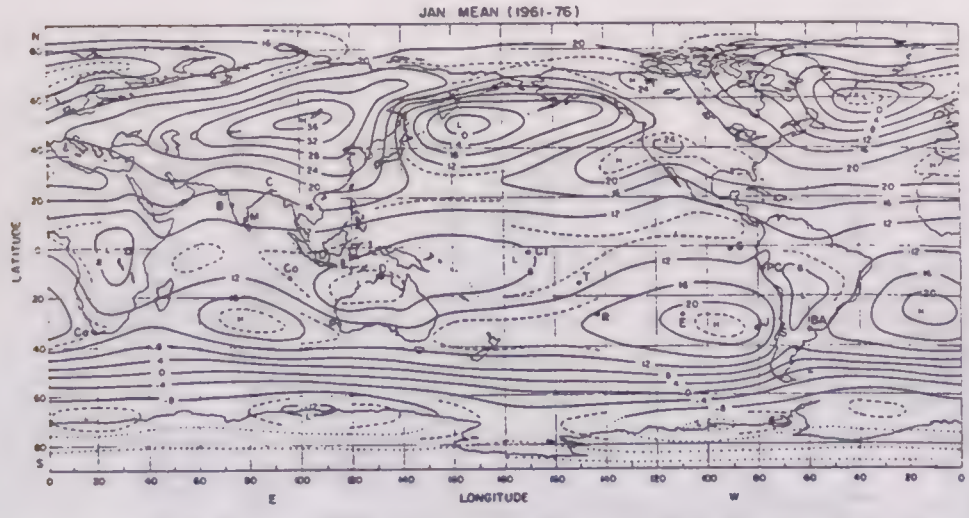


Figure 6.2B.
From Kousky et al (1984

January mean sea level pressure (1961–76). Adapted from Godbole and Shukla (1981). Stations commonly referred to as being key stations in the Southern Oscillation and indicated in the figure are: Capetown (Ca), Bombay (B), Madras (M), Calcutta (C), Djakarta (Dj), Darwin (D), Perth (P), Cocos Island (Co), Canton Island (CI), Papaete, Tahiti (T), Rapa (R), Easter Island (E), Juan Fernandez Island (J), Galapagos Islands (G), Puerto Chicama (PC), Santiago (S) and Buenos Aires (BA).

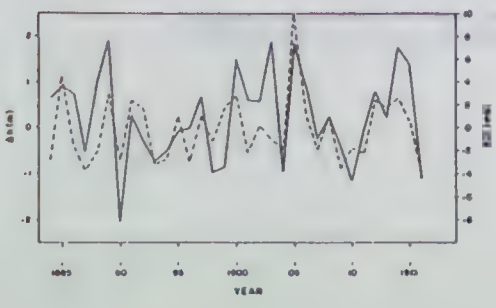


The mean Parana river level anomalies (m), for April–September, at Rosario, Argentina (dashed line) and a Southern Oscillation Index (SOI) (solid line) calculated by taking the sum of the pressure anomalies (mb) at Bombay, Madras, Djakarta, Calcutta, Darwin, Perth and Cape Town for the period of October–March. The SOI values are plotted in the year corresponding to the January–March period, and are taken from Berlage (1966). The Parana river level anomalies are taken from Mossman (1924).

Figure 6.3. From Kousky et al (1984).

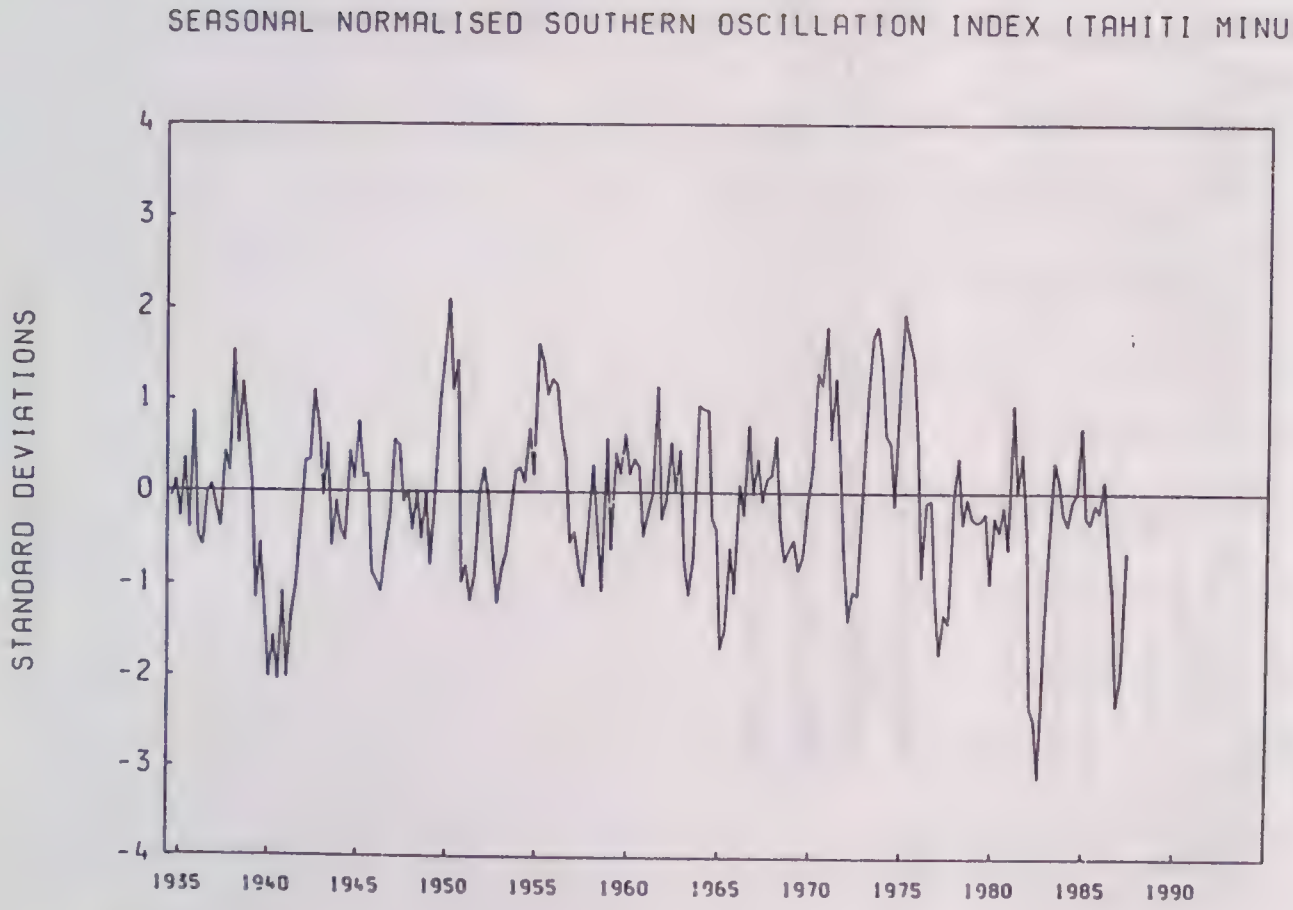
SEASONAL NORMALISED SOUTHERN OSCILLATION INDEX (TAHITI MINUS DARWIN)
STANDARD DEVIATIONS
4
3
2
1
0
-1
-2
-3
-4
1935
1940
1945
1950
1955
1960
1965
1970
1975
1980
1985
1990

Figure 6.4

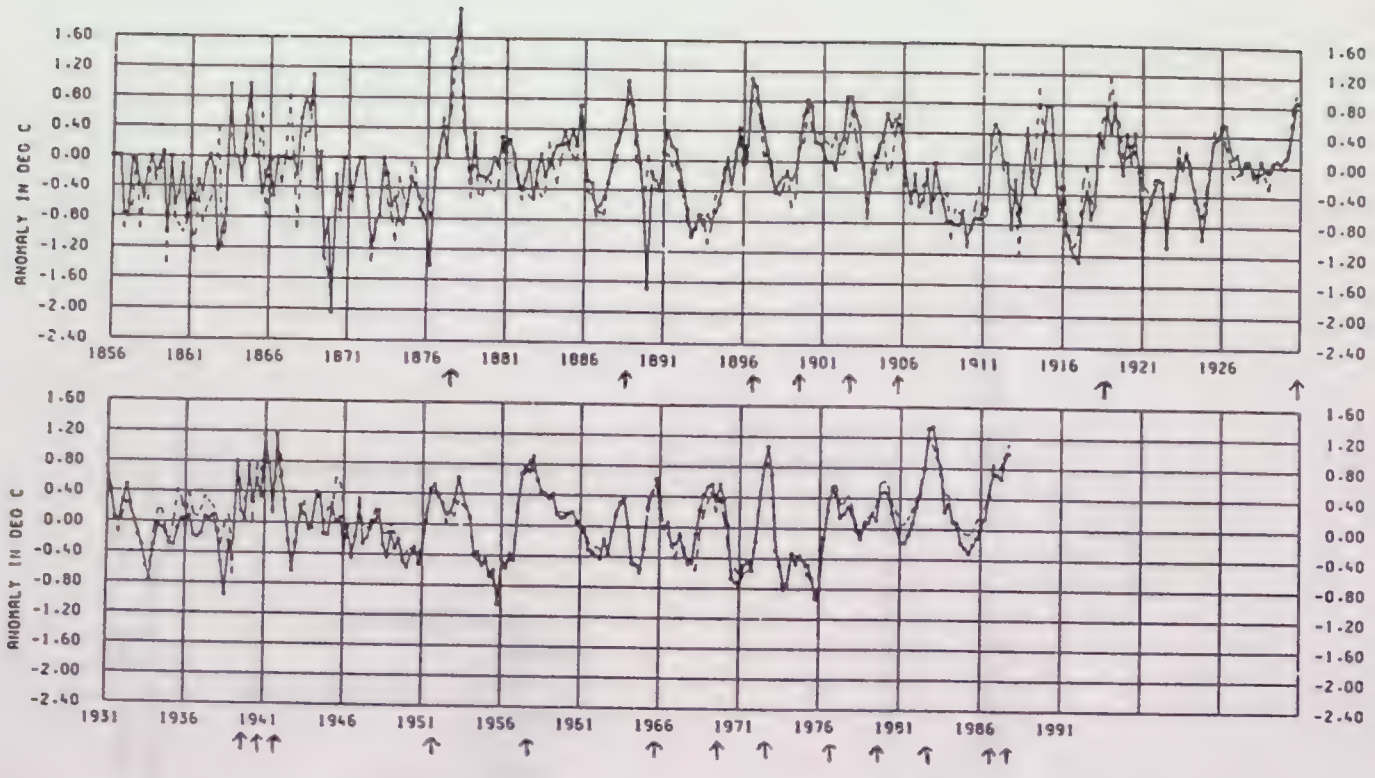


Figure 6.5. Seasonal sea surface temperature (solid) and night marine air temperature (dashed) anomalies (w.r.t. 1951-80) averaged over the tropical East Pacific (20°N to 20°S, east of 170°W) , 1856 to 1987. Arrows mark Oct to Dec of El Nino years.

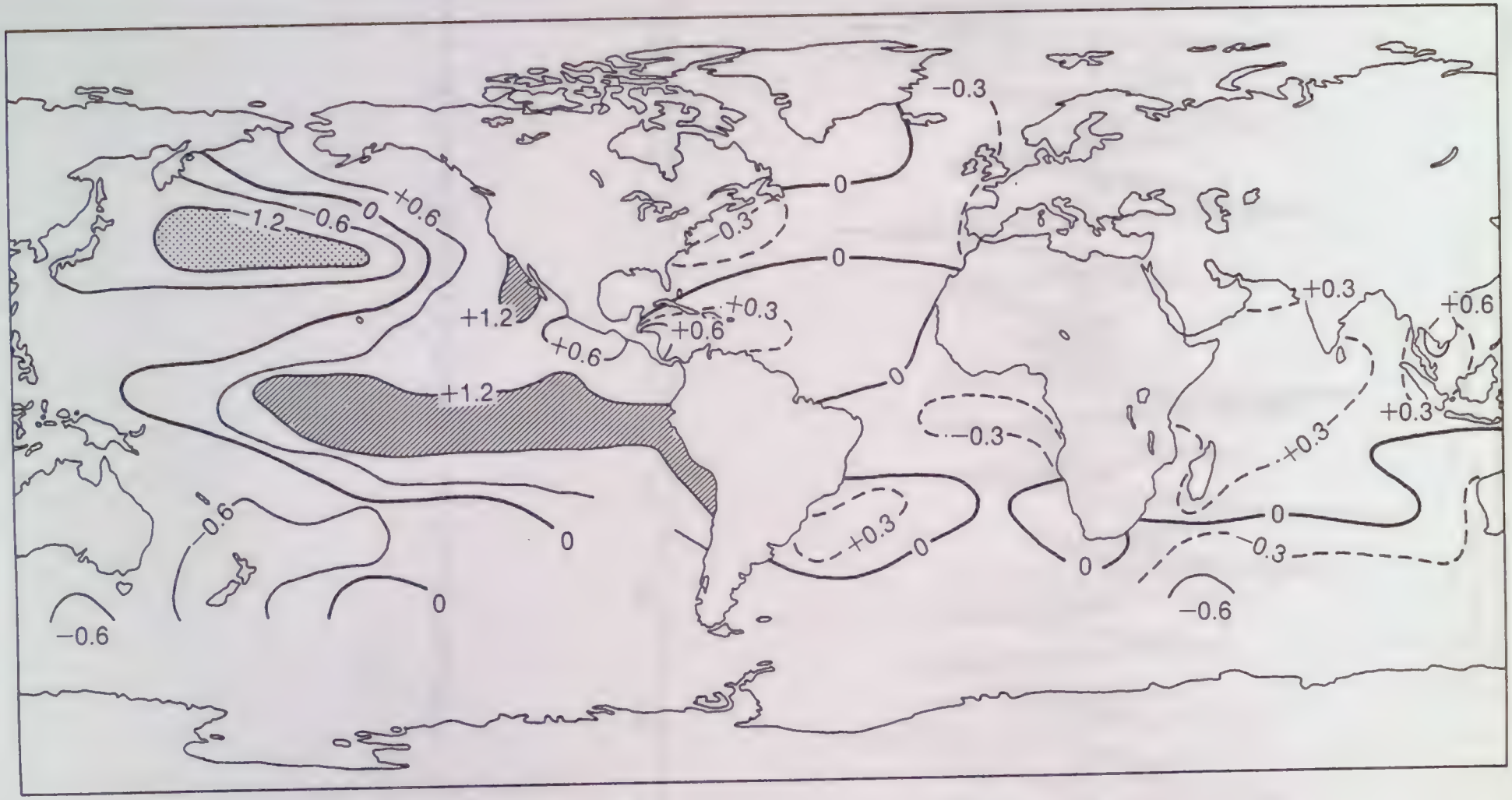


Figure 6.6 The second covariance matrix eigenvector (EOF2) of worldwide SSTA, 1901-80.
The values are normalised so that the sum of the squares of the values for $10^{o}$ squares is 100.

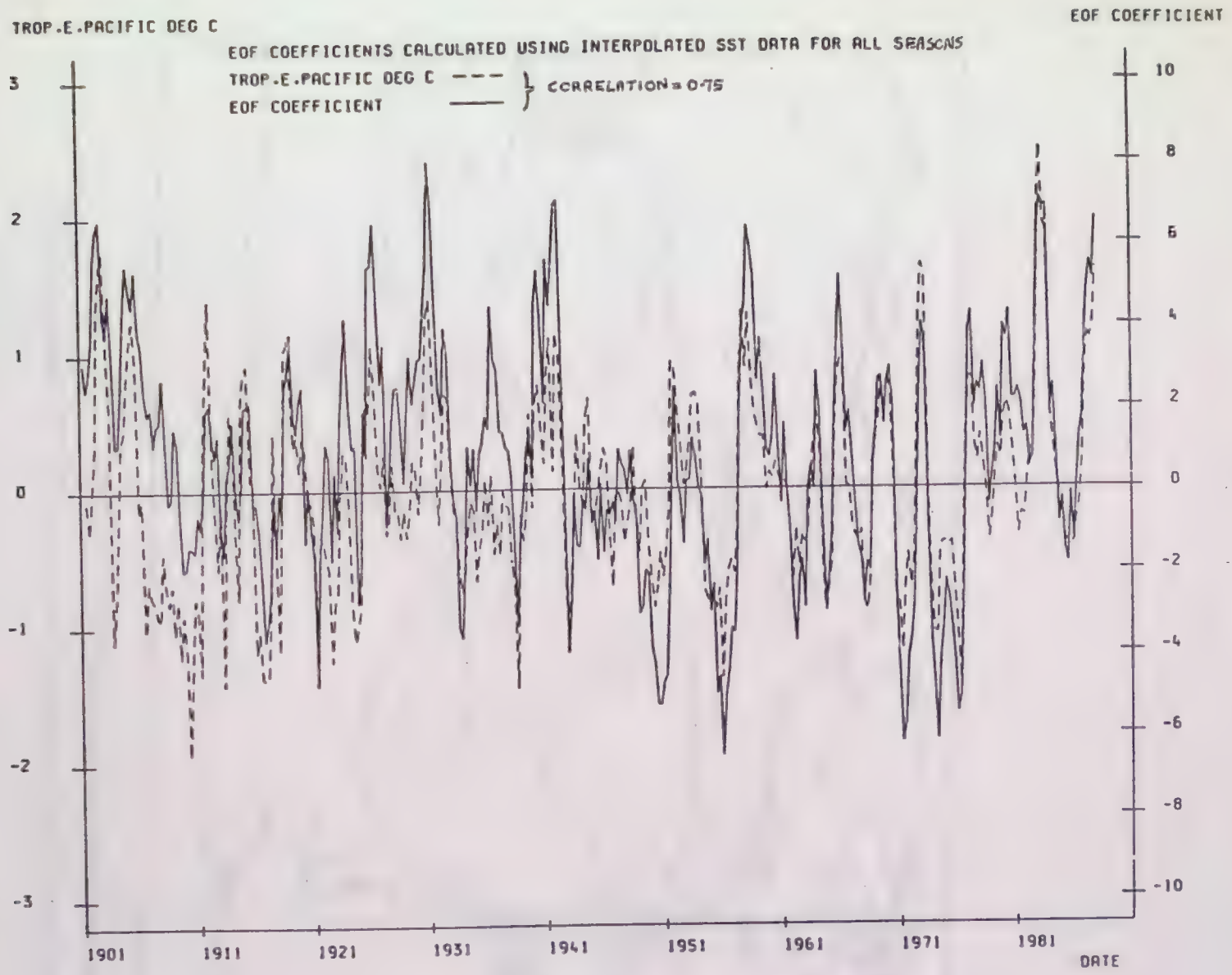


Figure 6.7. Comparison between EOF 2 coefficient and Tropical East Pacific SSTA time series.

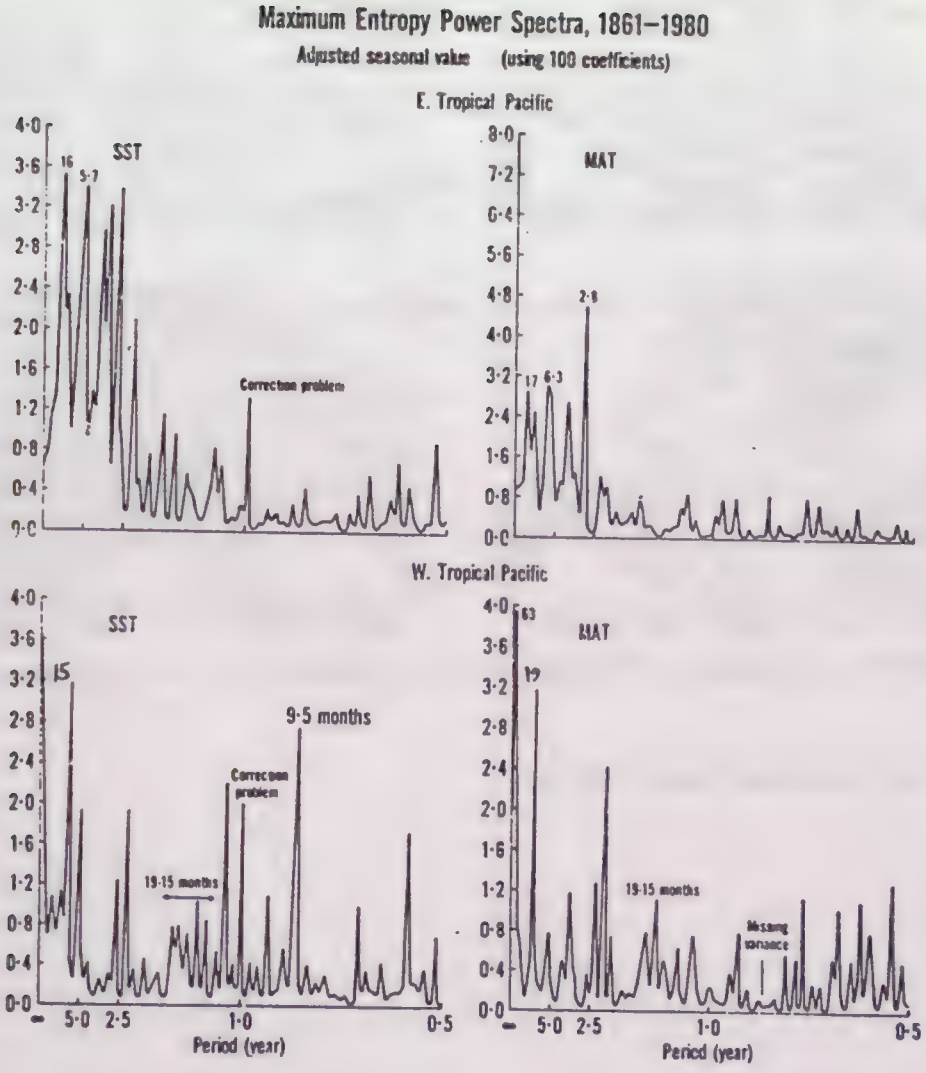


Figure 6.8. From Folland et al (1985).

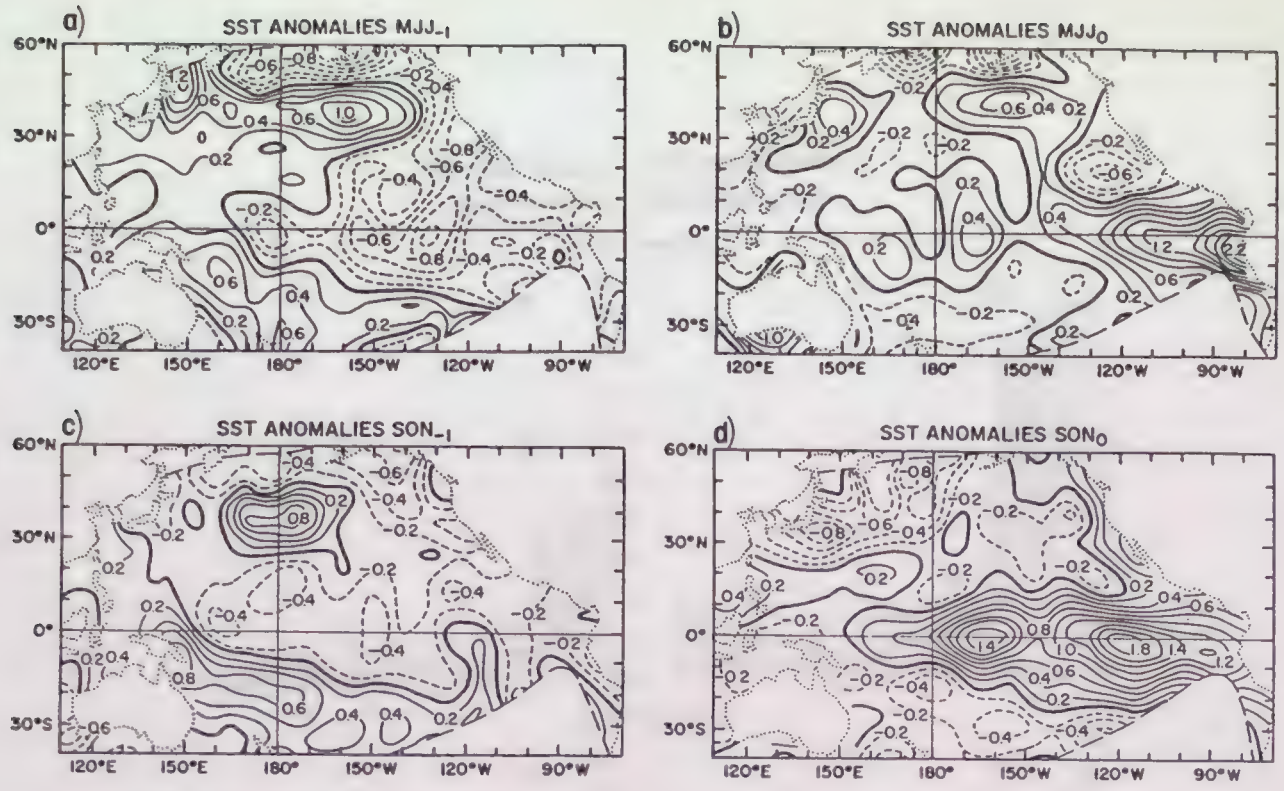


Anomalies of sea surface temperature (°C) in a) May–Jun–Jul$_{-1}$; b) May–Jun–Jul$_0$; c) Sep–Oct–Nov$_{-1}$; d) Sep–Oct–Nov$_0$.

Figure 6.9 From van Loon and Shea (1987).

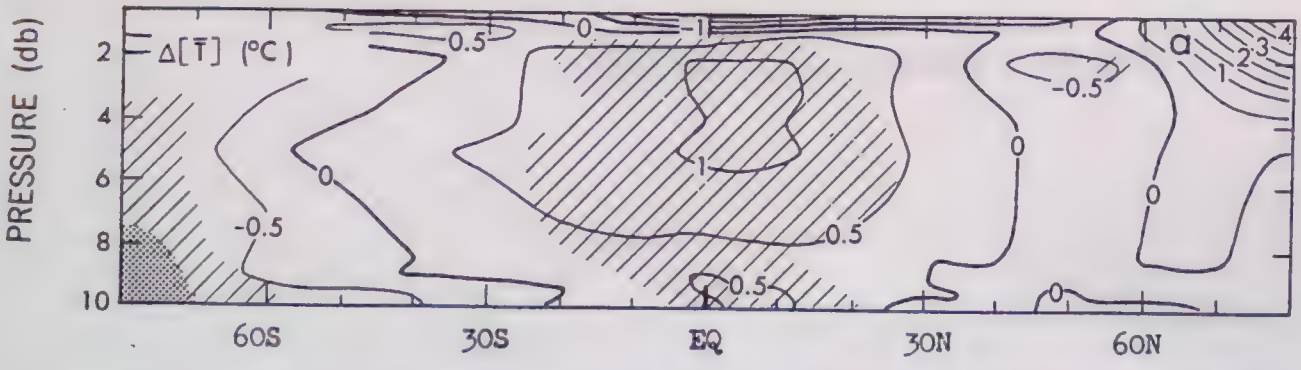


Figure 6.10. Zonal mean cross section of the average temperature difference (°C) between cases when the Dec to Feb surface temperature at 2.5°S,130°W was relatively high and cases when it was relatively low.

After Pan and Oort (1983).

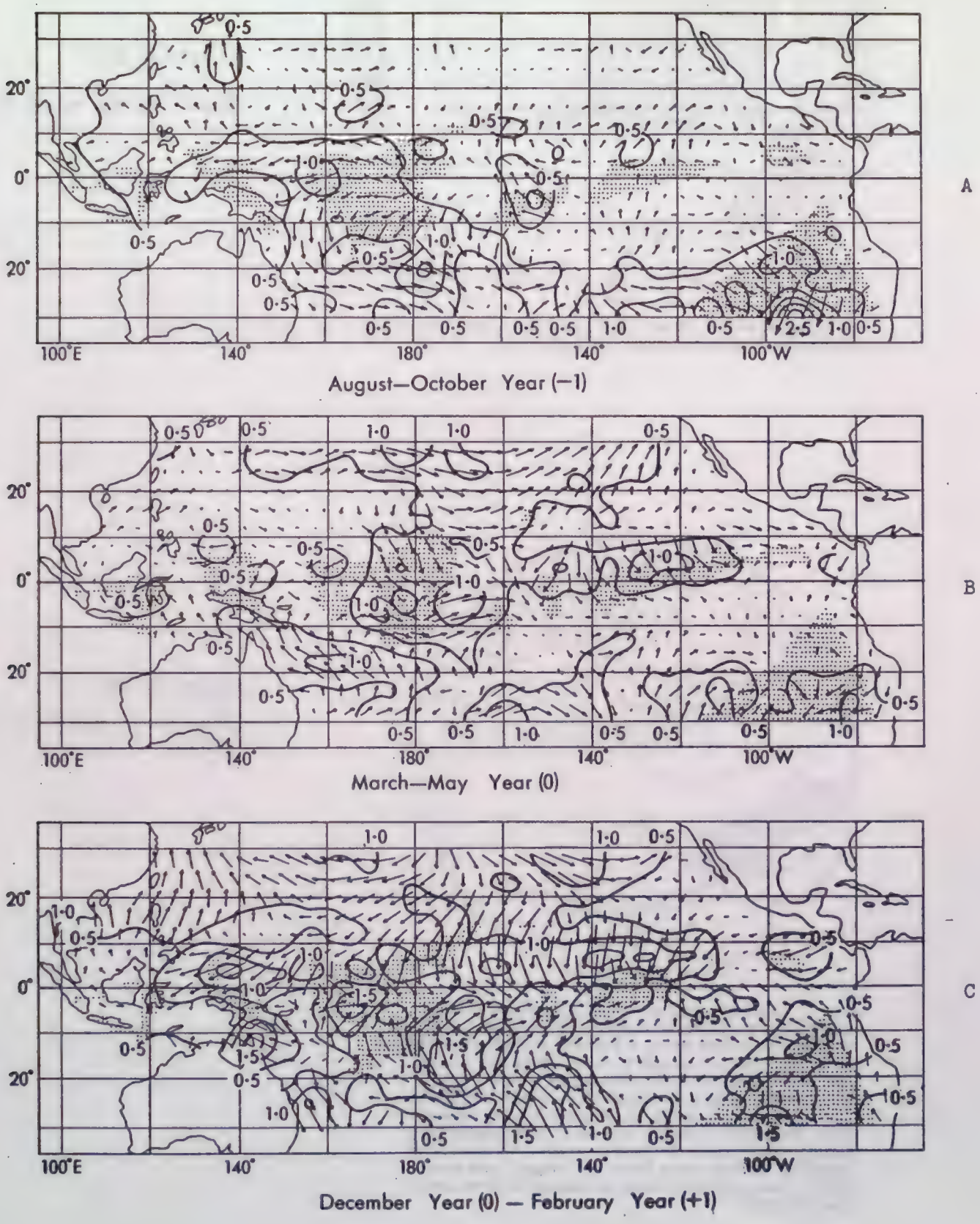


El-Nino surface wind anomaly composites (units m $s^{-1}$).

Areas in which the number of observations average less than 10 in a two degree square are shaded on the wind composite.

Figure 6.11. After Rasmusson and Carpenter (1982).

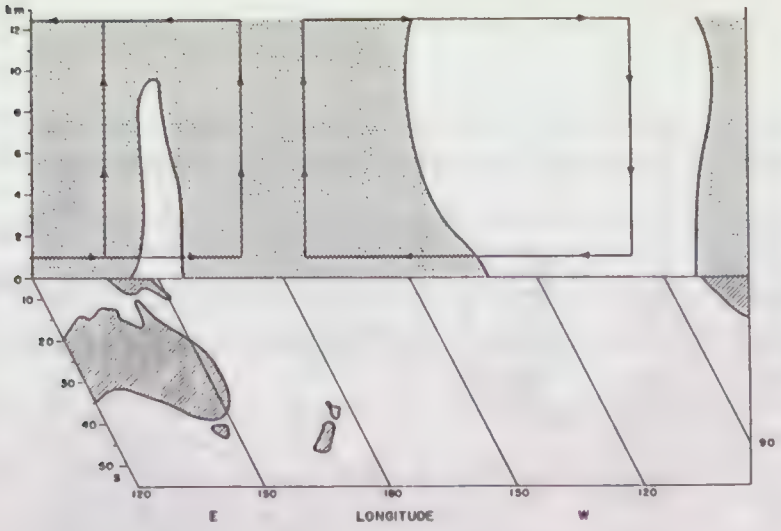


Figure 6.12A.

From Kousky et al (1984).

Schematic diagram of the Pacific Walker Circulation. Shaded regions are areas of rising motion. The circulation pattern shown is the January mean for 1979–81.

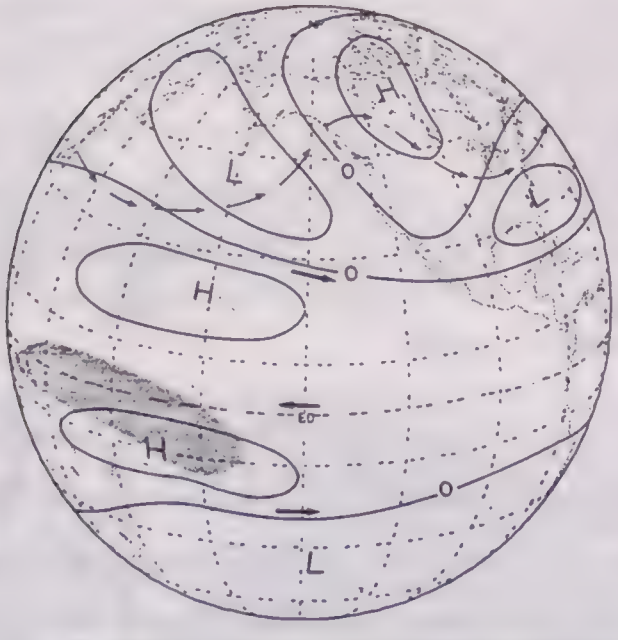


Figure 6.12B.

After Horel and Wallace (1981).

Schematic illustration of the hypothesized global pattern of middle and upper tropospheric geopotential height anomalies (solid lines) during a Northern Hemisphere winter which falls within an episode of warm sea surface temperatures in the equatorial Pacific. The arrows in darker type reflect the strengthening of the subtropical jets in both hemispheres along with stronger easterlies near the equator during warm episodes. The arrows in lighter type depict a mid-tropospheric streamline as distorted by the anomaly pattern, with pronounced "troughing" over the central Pacific and "ridging" over western Canada. Shading indicates regions of enhanced cirriform cloudiness and rainfall.

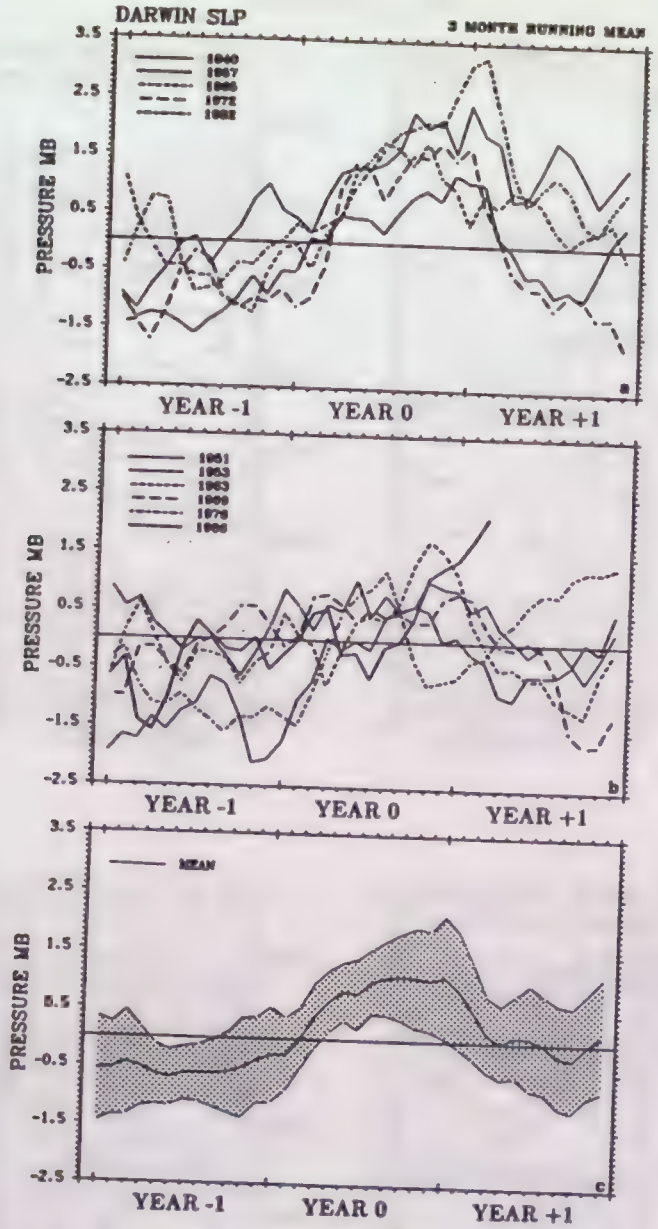


Sequences of anomalies in sea level pressure at Darwin over all El Niño events since 1939 from the year before (year −1) to the year following (year +1) the event. Each event is labeled by the central year (year 0). The larger events are shown in (a), the smaller events in (b), and the composite mean (excluding 1986) plus and minus one standard deviation is given in (c).

Figure 6.13 From Trenberth and Shea (1987)

MSL PRESSURE

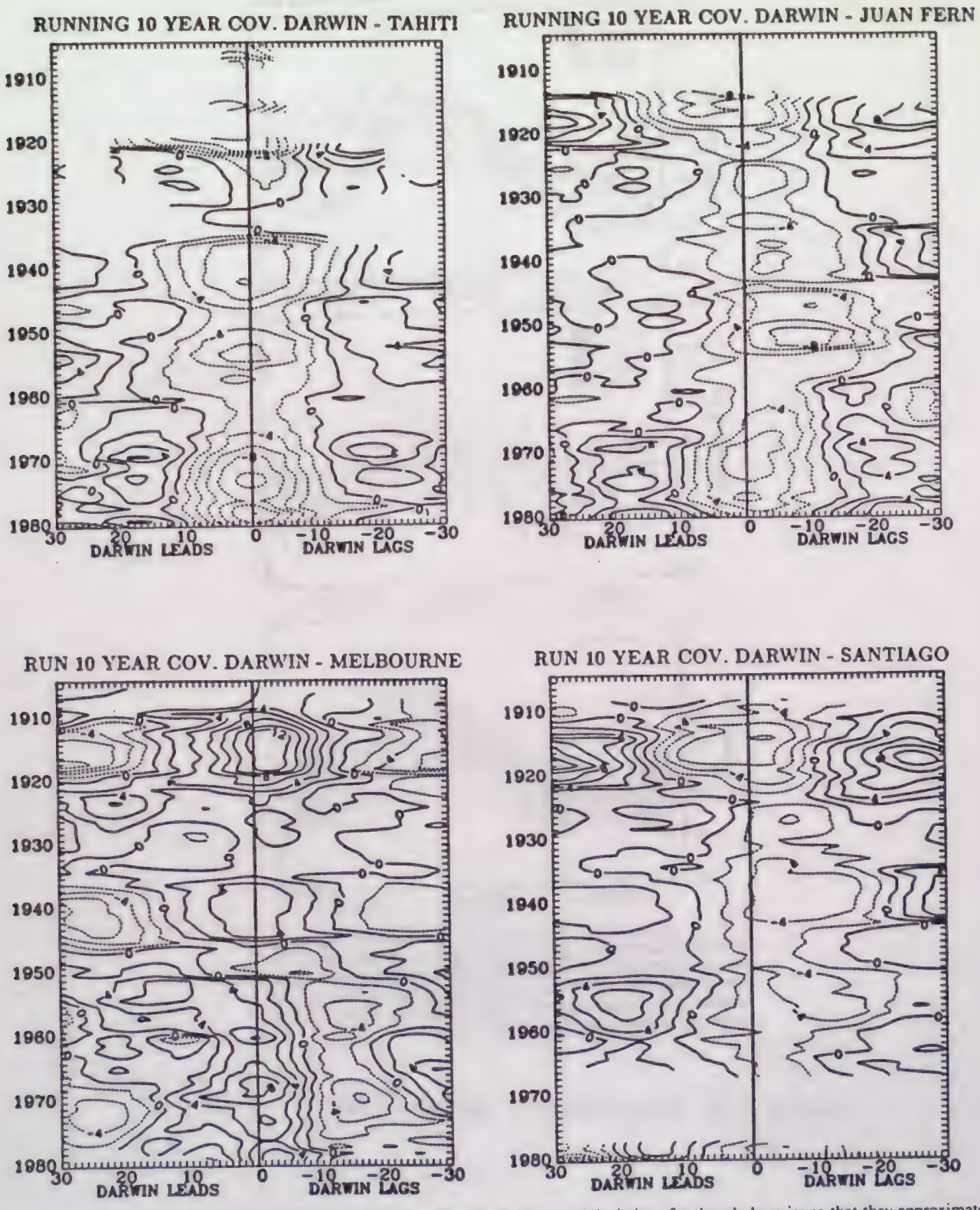


Ten-year running cross covariances (×10) normalized by the standard deviations for the whole series so that they approximate correlations, as a function of lag up to ±30 months, of Darwin with Tahiti, Juan Fernandez, Melbourne and Santiago for 1900–84. Missing data areas are left blank.

Figure 6.14 From Trenbeth and Shea (1987).

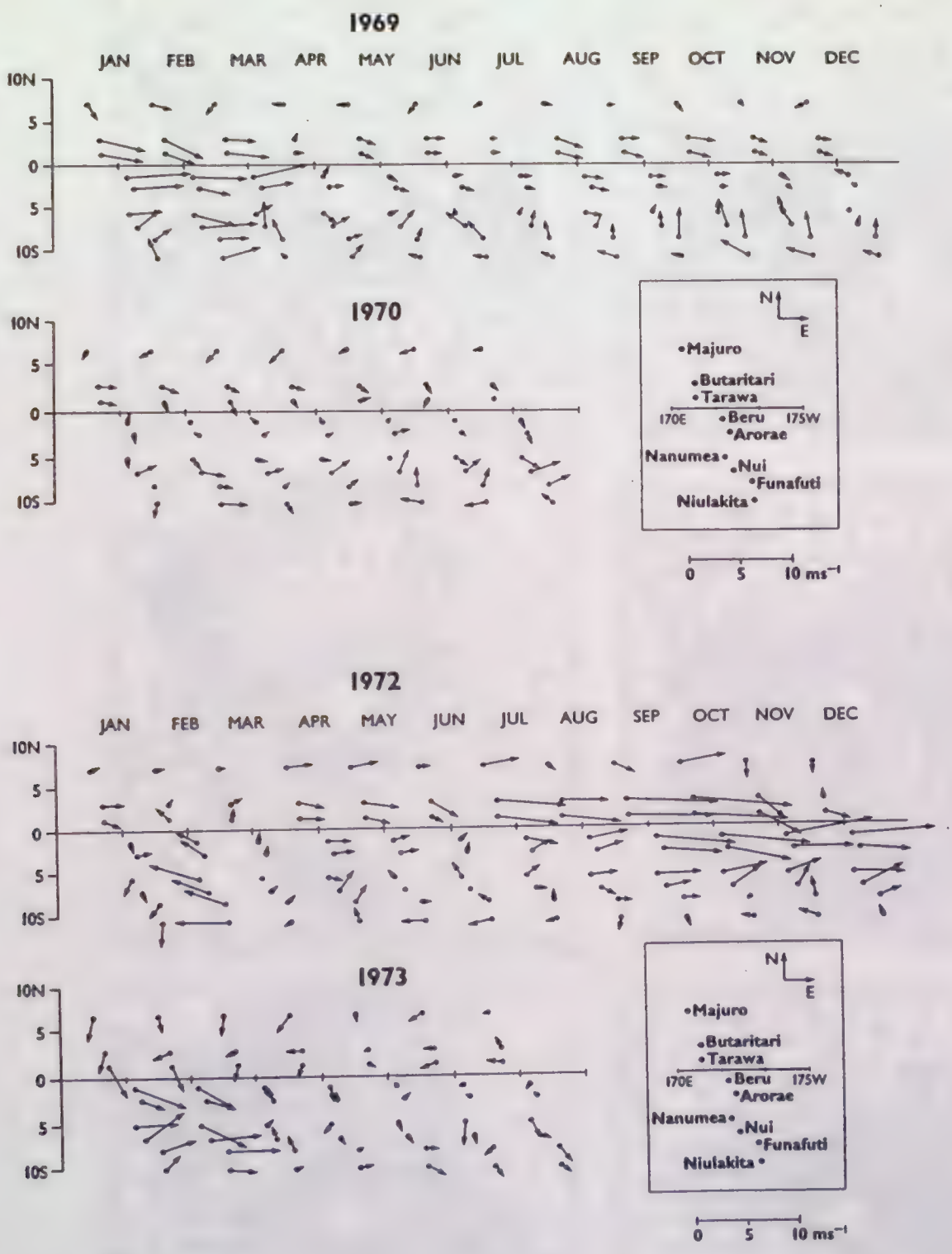


Figure 6.15 Monthly mean wind anomalies for the El Nino periods of 1969-70 and 1972-3.. From Harrison (1987).

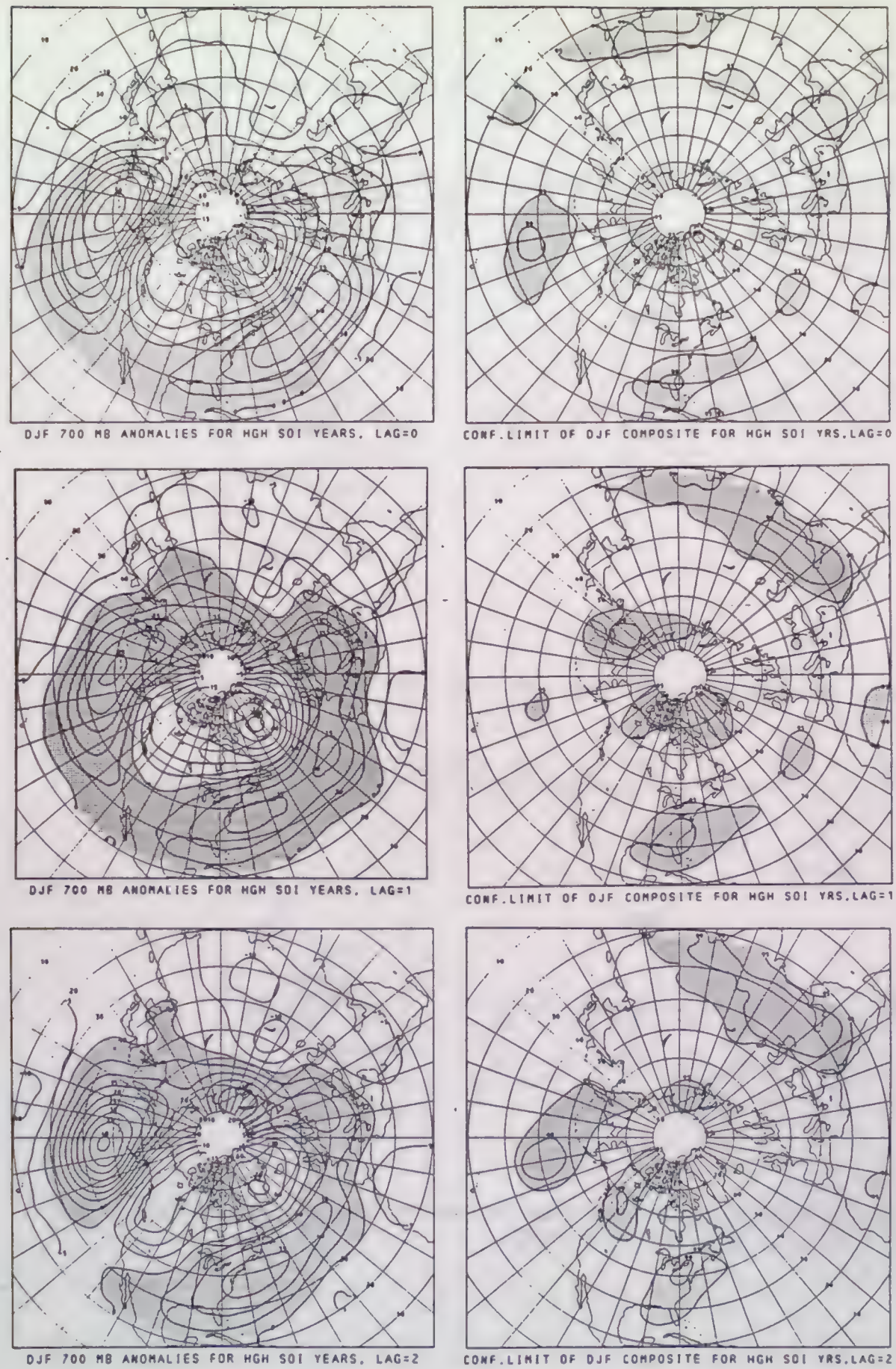


Winter composites associated with high SOI values with the latter leading the height field by various seasons. The shaded areas are positive and the contour interval is 5 m. Confidence limits of the anomalies are presented on the right.

Figure 6.16A. From Chen (1982).

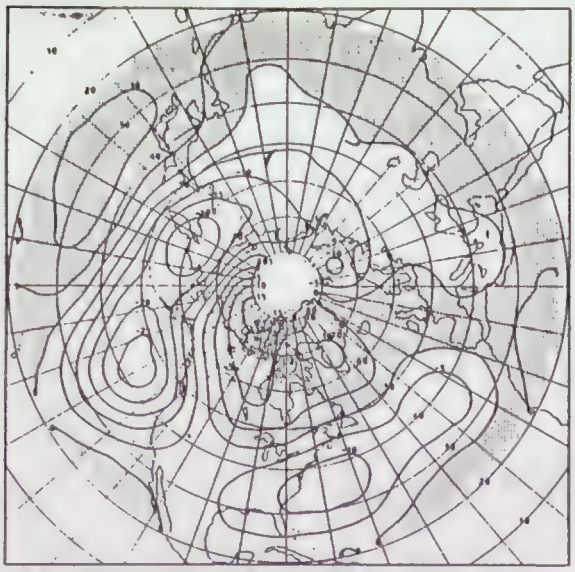


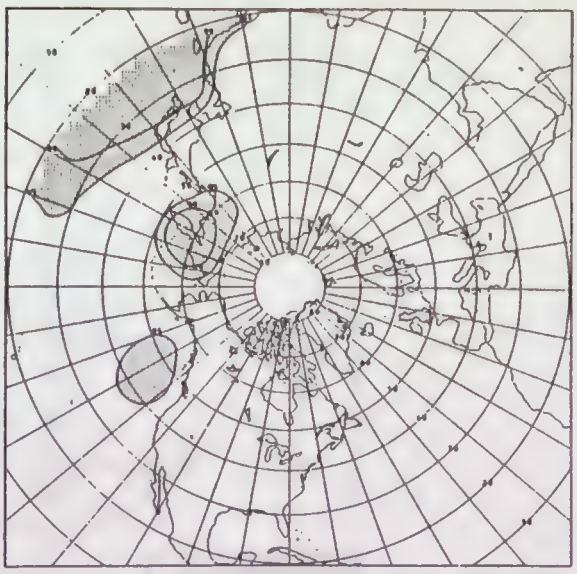


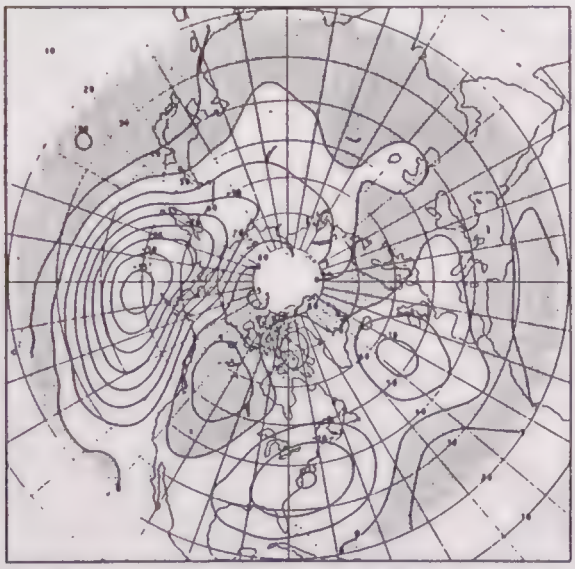


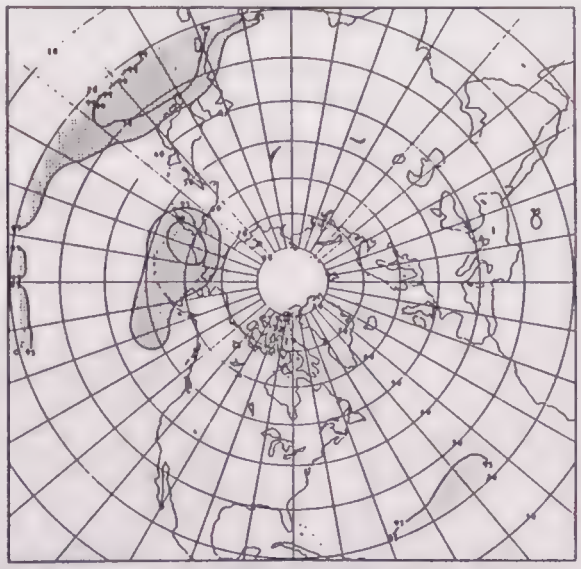


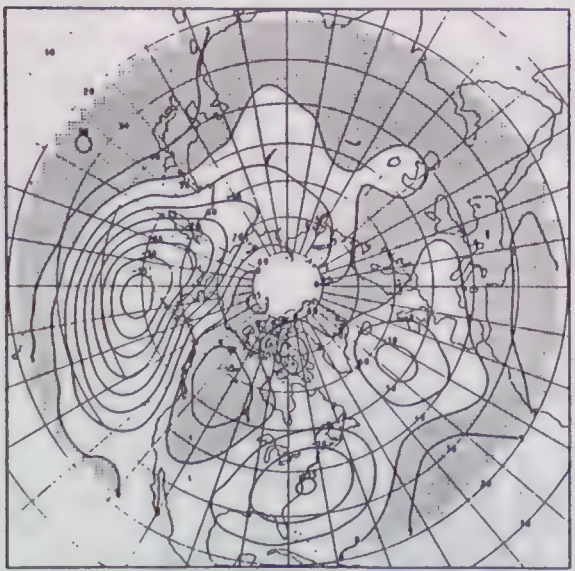


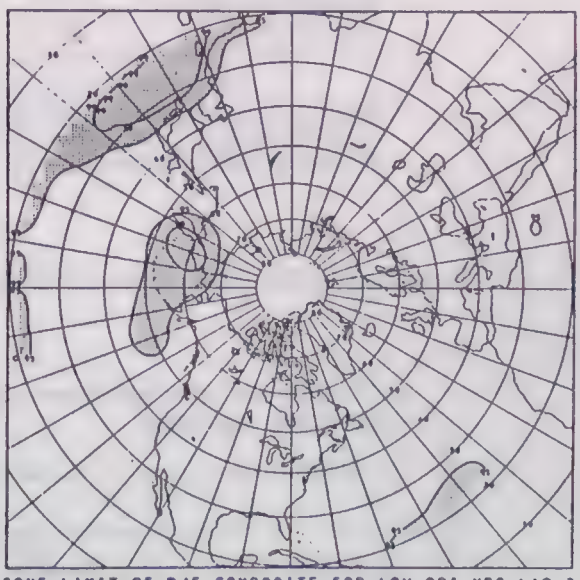


Figure 6.16B. As Fig. 6.16A, but for low SOI values.
From Chen (1982).

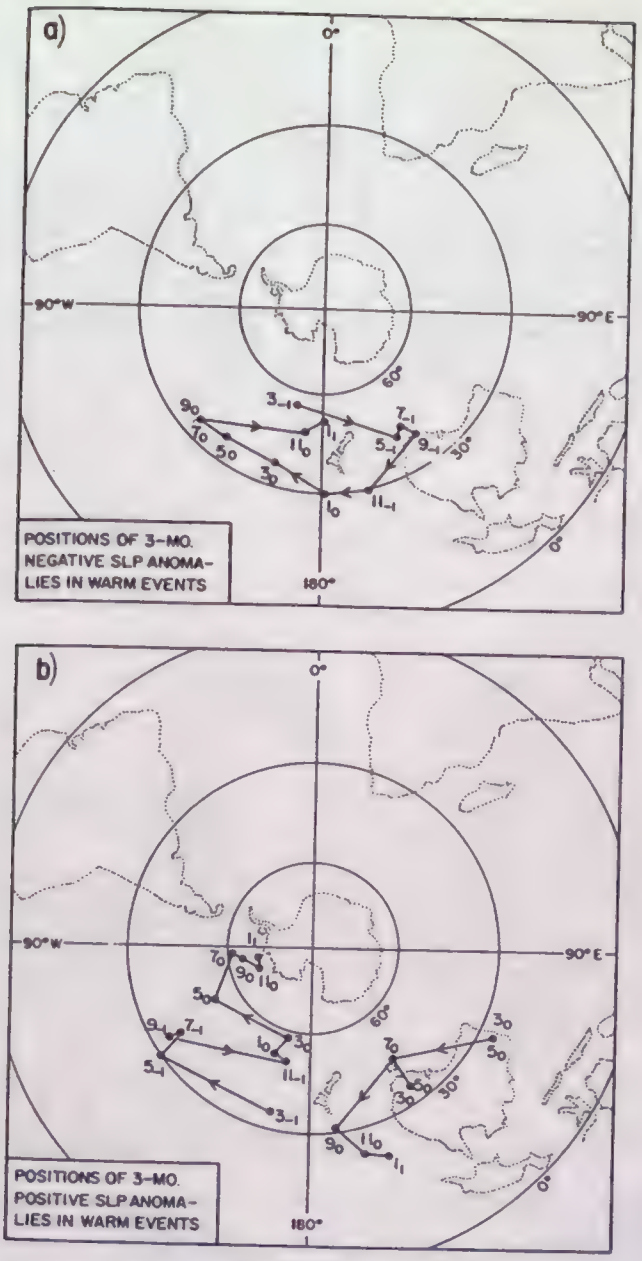


The movement of the major three-month average anomalies of sea level pressure. The averages overlap by one month: $3_{-1}$ is Feb–Mar–Apr of Year$_{-1}$ and $5_{-1}$ is Apr–May–Jun of Year$_{-1}$. b) As in Fig. a, but for positive anomalies.

Figure 6.17 From van Loon and Shea (1987).

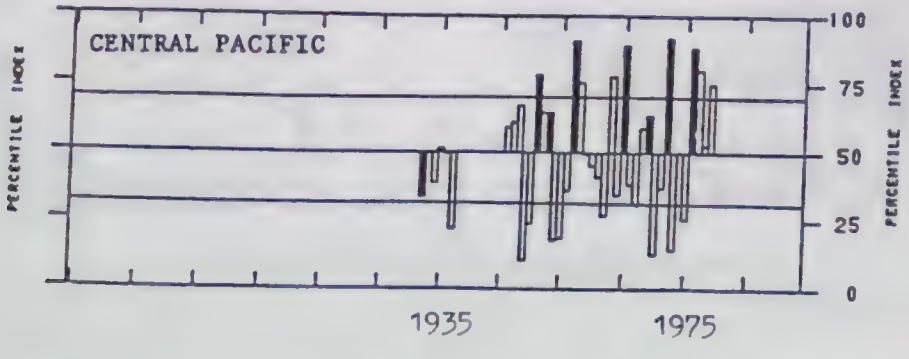


Figure 6.18 Central Pacific rainfall series from Ropelewski and Halpert (1987). El Nino years are shaded.

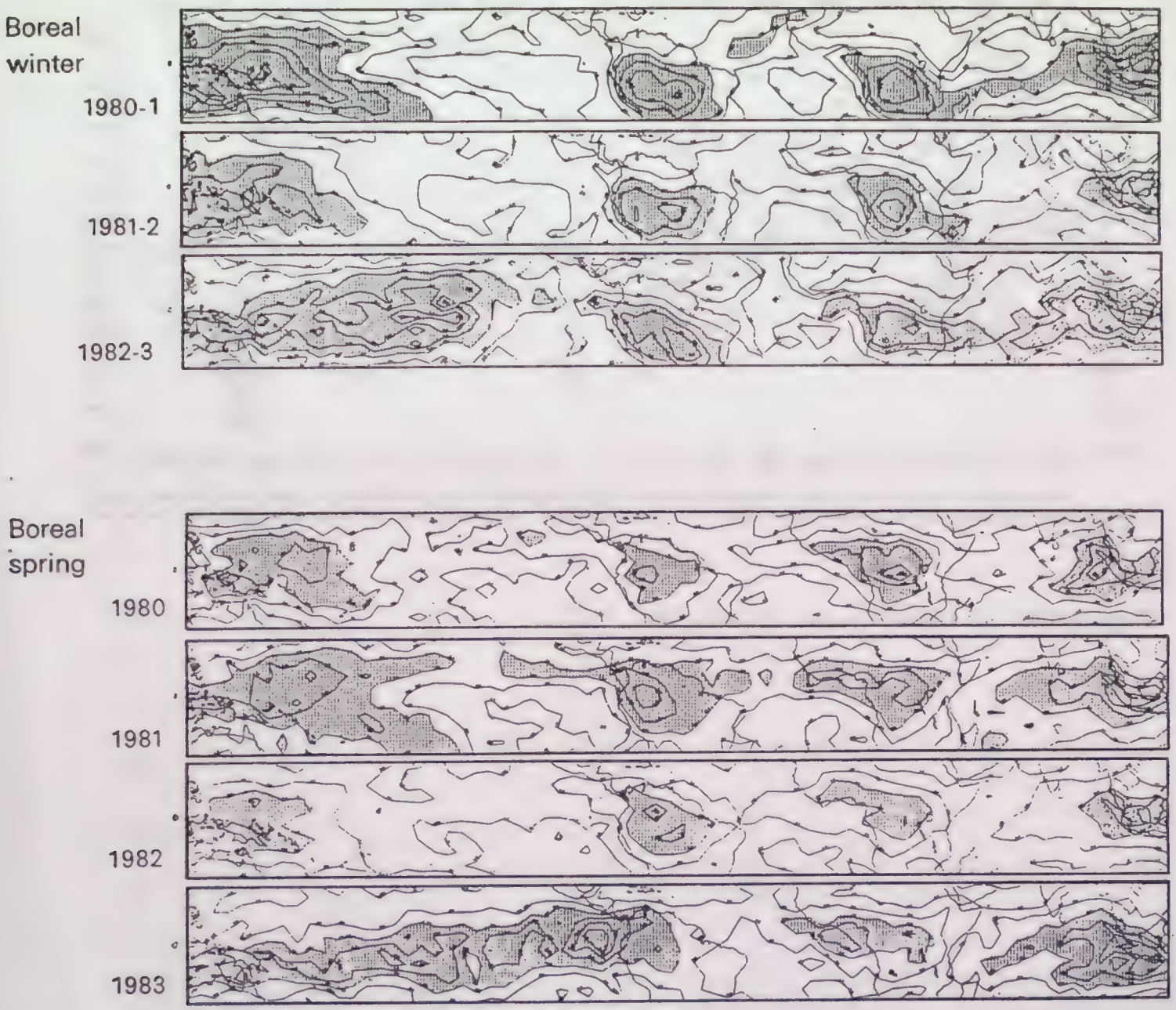


Percentage cover of cloudtops with radiative temperatures less than 235° K. Contours drawn at 10% intervals. Areas of ≥30% cloud cover are shaded.

Figure 6.19. From Newman (1984).

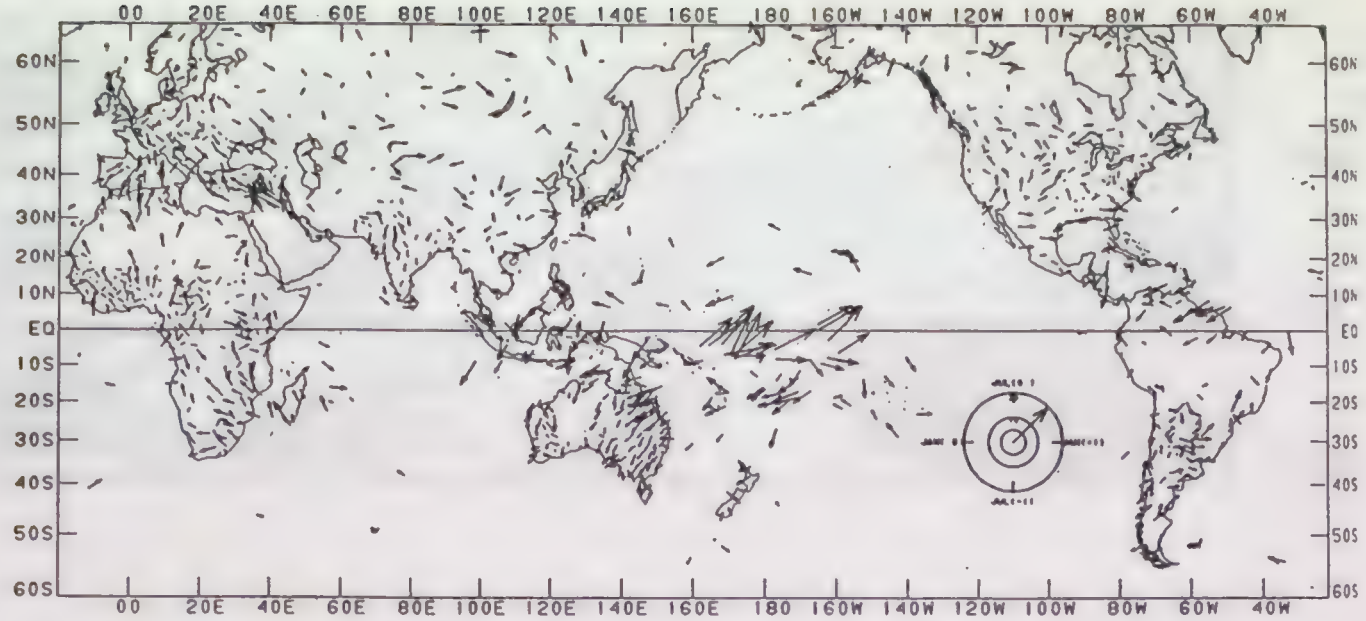


The amplitudes and phases of ENSO composite ranked precipitation plotted as vectors. The vectors are based on a 24-month harmonic fitted to ranked precipitation composites for ENSO episodes. The phases and relative magnitudes of these vectors are indicated by the "vector clock" in the figure.

Figure 6.20 From Ropelewski and Halpert (1987).

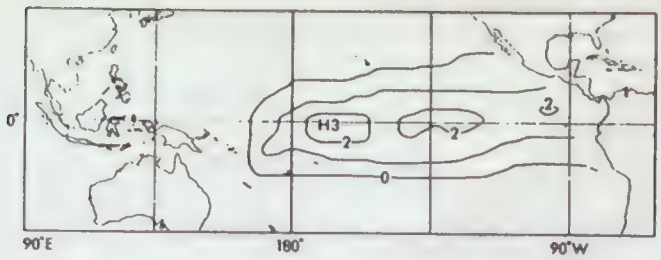


Figure 6.21A. Composite El Nino SSTA (°C) used by Palmer and Mansfield (1986a).

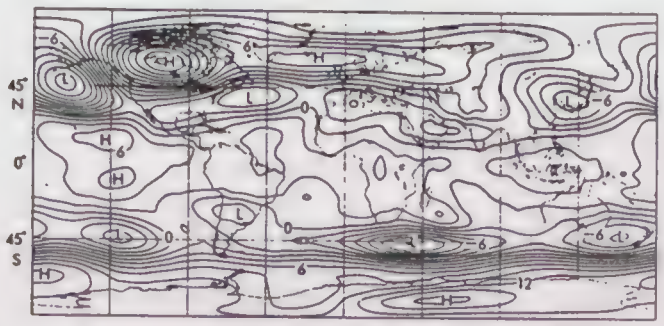


Figure 6.21B. Anomalous 250mb height (dam) for above composite SSTA. From Palmer and Mansfield (1986a).

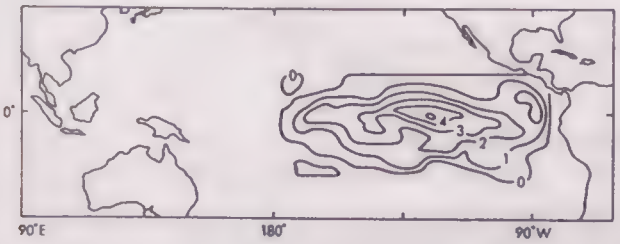


Figure 6.21C. El Nino SSTA (°C) for December 1982 used by Palmer and Mansfield (1986b).

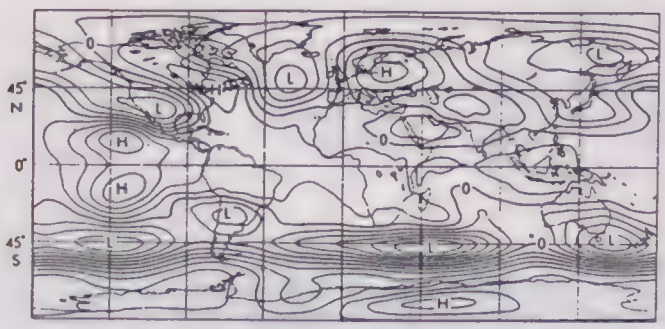


Figure 6.21D. Anomalous 250mb height (contours every 2 dam) for SSTA in Figure 6.21C and envelope orography. From Palmer and Mansfield (1986b).

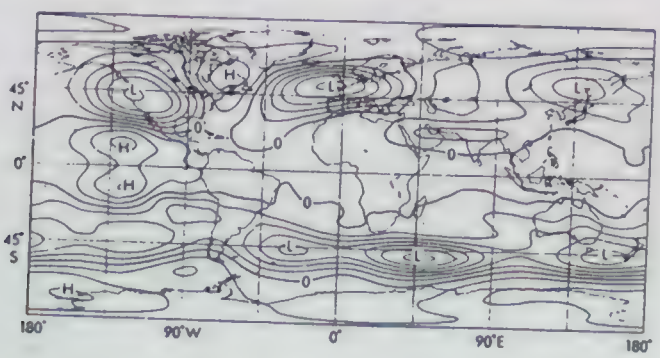


Figure 6.21E.
As Fig. 6.21D but using standard orography.

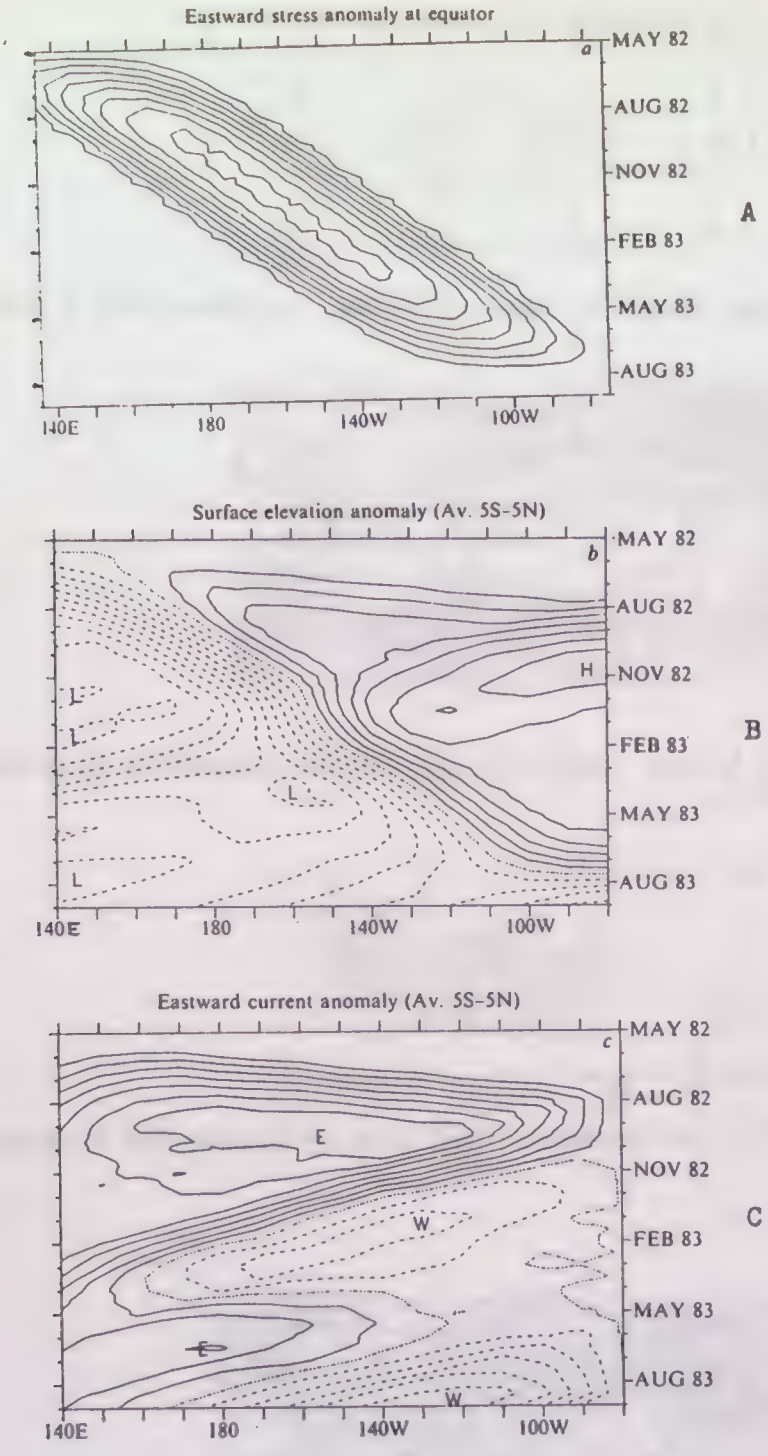


Longitude–time plots along the Equator of A, eastward stress anomaly, B, surface elevation and C, zonal surface current. Values are averages between 5° S and 5° N. B and C are the results of a model calculation in which A is the forcing function. Solid contours represent positive values and broken contours negative values.

Figure 6.22. From Gill and Rasmusson (1983).

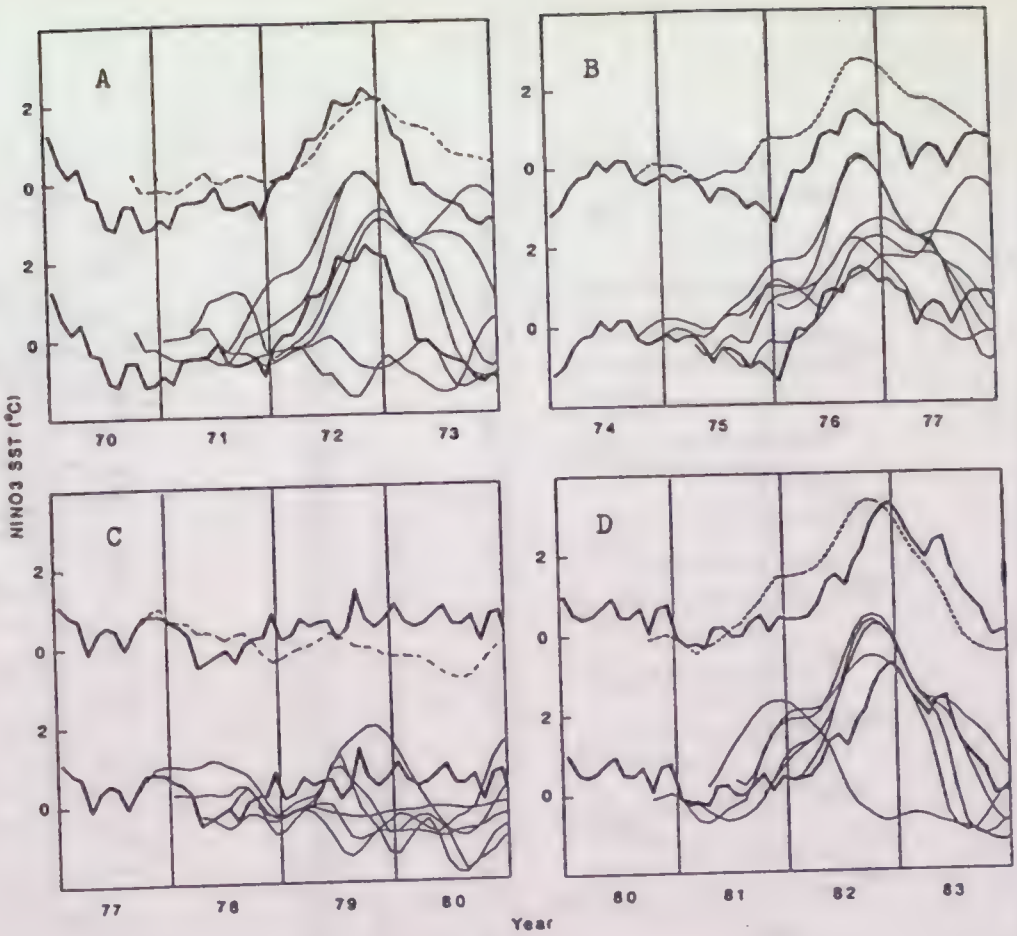


SST anomalies (°C) averaged over the eastern equatorial Pacific NINO3 region (90° W to 150° W, 5° S to 5° N) for four periods centred on 1972, 1976, 1979 and 1982. Heavy curves, observed values as reported by CAC/NOAA (note repetition of vertical scale). Light curves, values from six forecasts initiated at 3-month intervals from the October two years ahead to the January of the nominal year. Dashed curve, average of the six forecasts (the consensus forecast).

Figure 6.23 From Cane et al (1986).

A

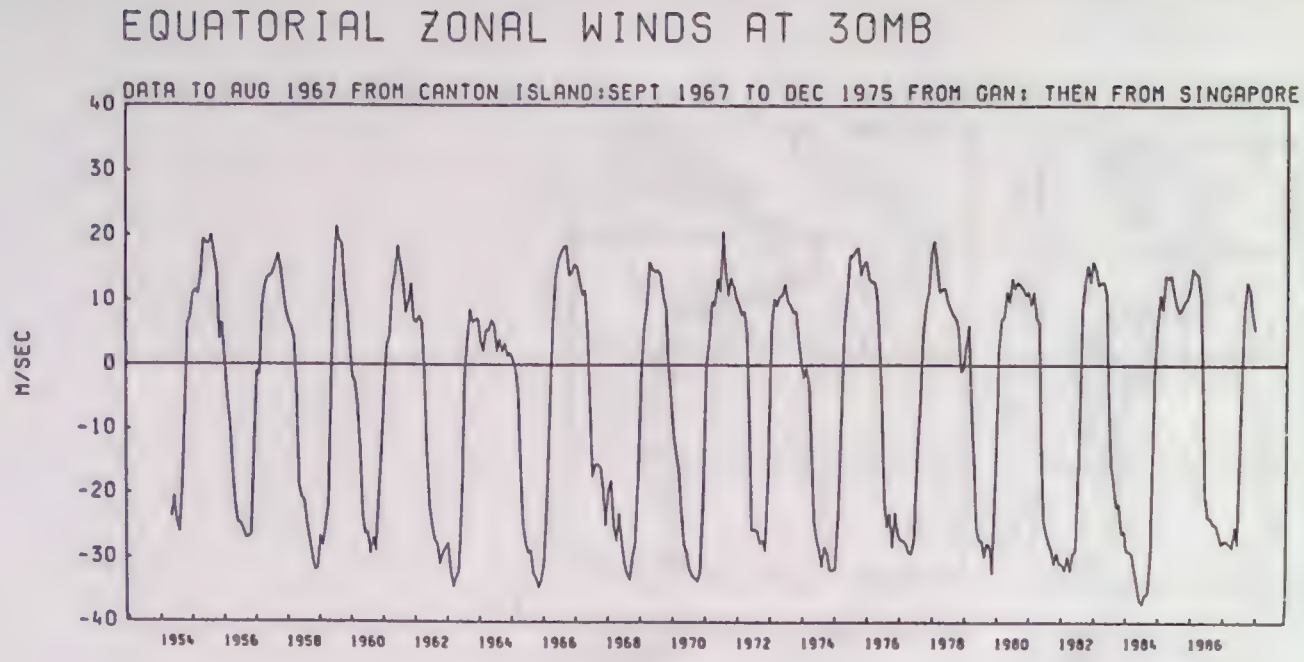


Figure 6.24.

B

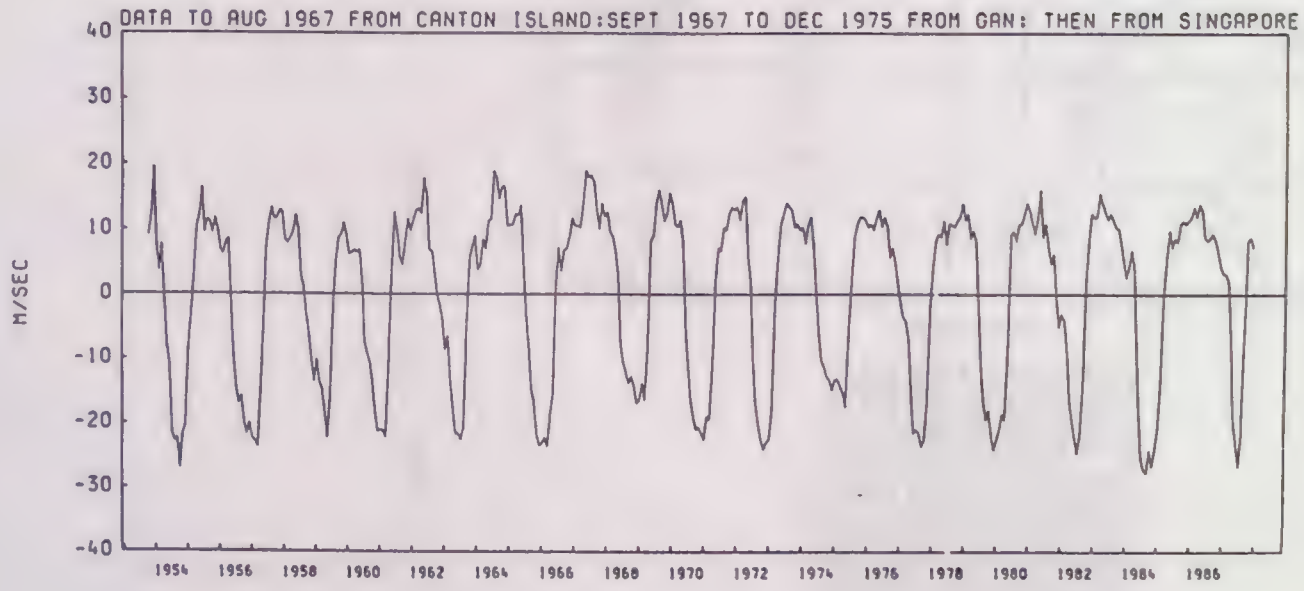

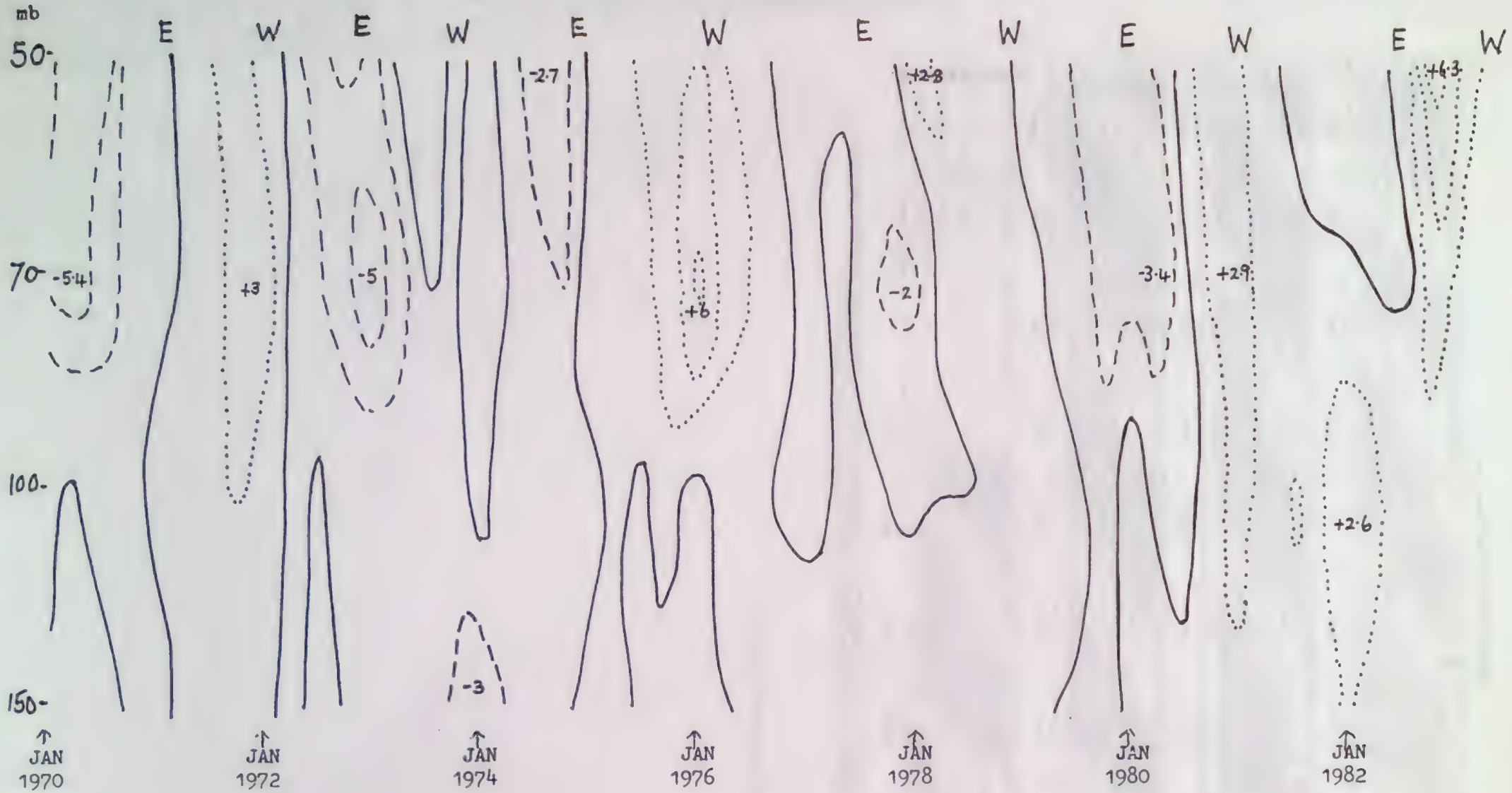


Figure 6.25. Temperature anomalies (w.r.t. 1971-80 average) over Singapore. Isotherms at 2°C intervals.

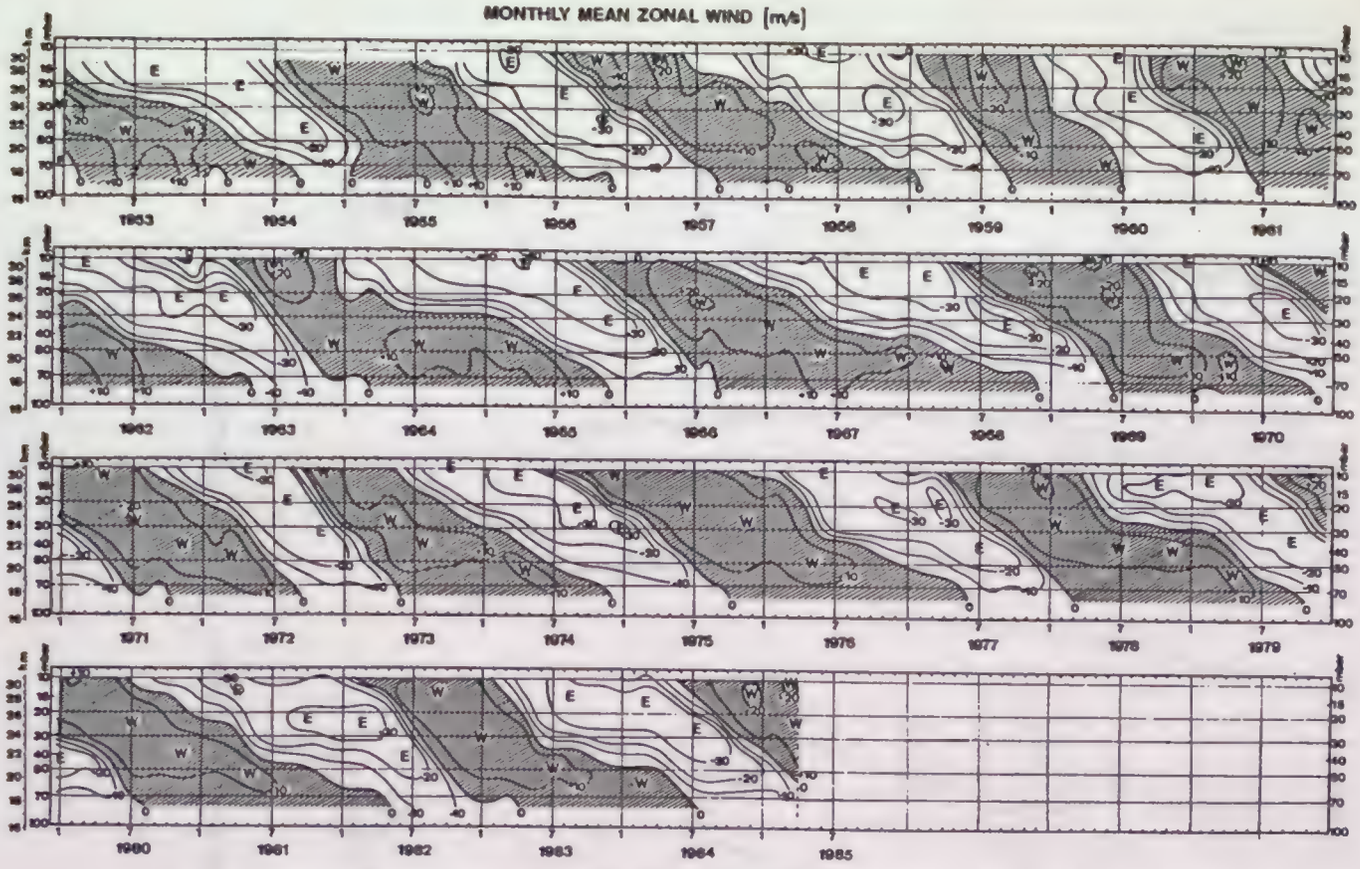


Time–height section of the monthly mean zonal wind components (m $s^{-1}$) at Canton Island (Jan 1953–Aug 1967), Gan/Mal ilive Islands (Sep 1967–Dec 1975), and Singapore (Jan 1976–Apr 1985).

Figure 6.26. From Naujokat (1986).

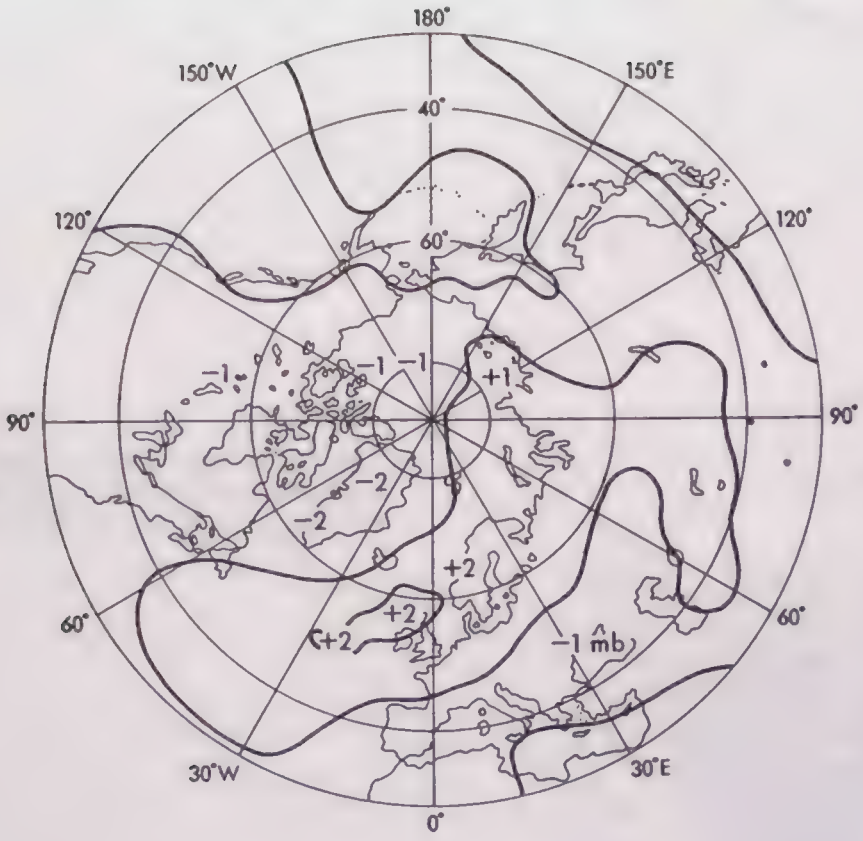


Surface pressure anomaly from 1951—70 average, July.
After Ebdon (1975).
Mean of eight Julys with westerly phase of QBO at 30 mb.

Figure 6.27.

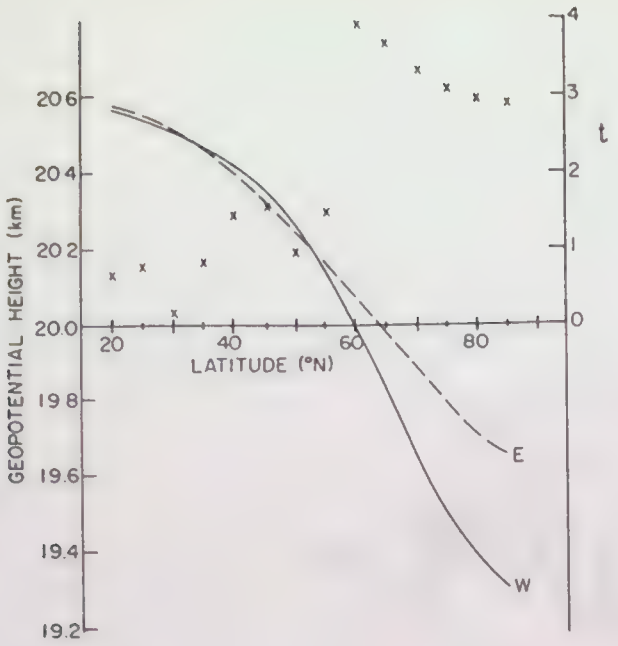


A. Composite meridional profiles of the zonal mean 50mb geopotential height for January to March. W and E denote westerly and easterly categories of equatorial 50mb QBO. Crosses denote Student's t values (right hand scale). t values of 2.16, 3.01, and 4.22 correspond to significance levels of 5%, 1% and 0.1% (13 degrees of freedom).

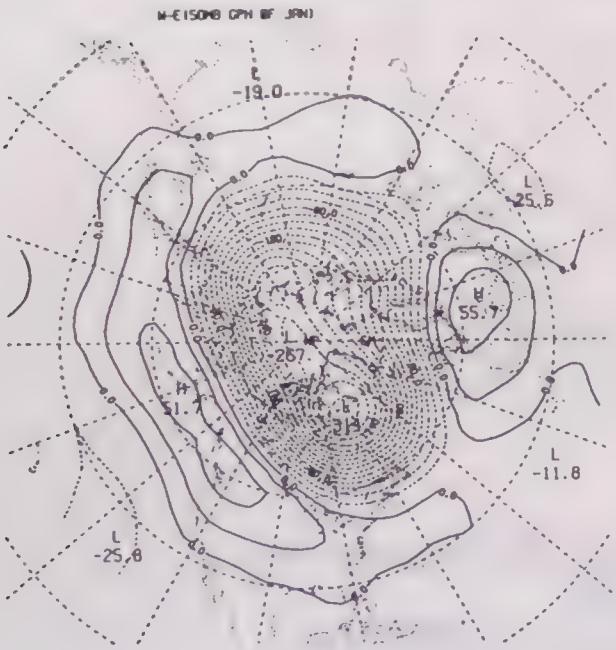

B. Monthly mean 50mb geopotential height difference (westerly minus easterly category of equatorial 50mb QBO) for January (gpm).

C. As B but for 1000mb geopotential height.

Figure 6.28. From Holton and Tan (1980).

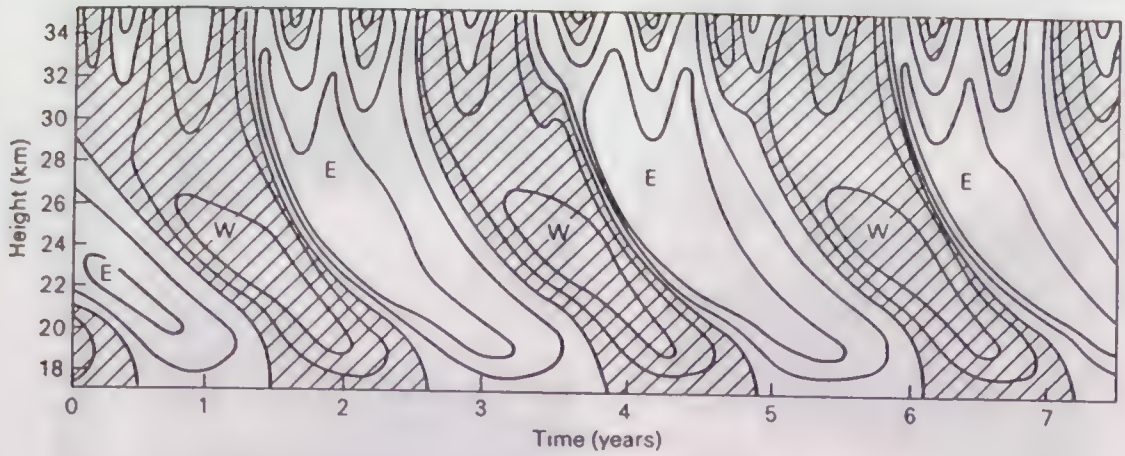


Time-height cross-section of mean zonal wind. After the model of Holton and Lindzen (1972).
Isopleths are drawn at 10 m $s^{-1}$ intervals.
Regions of westerly flow are shaded.

Figure 6.29.

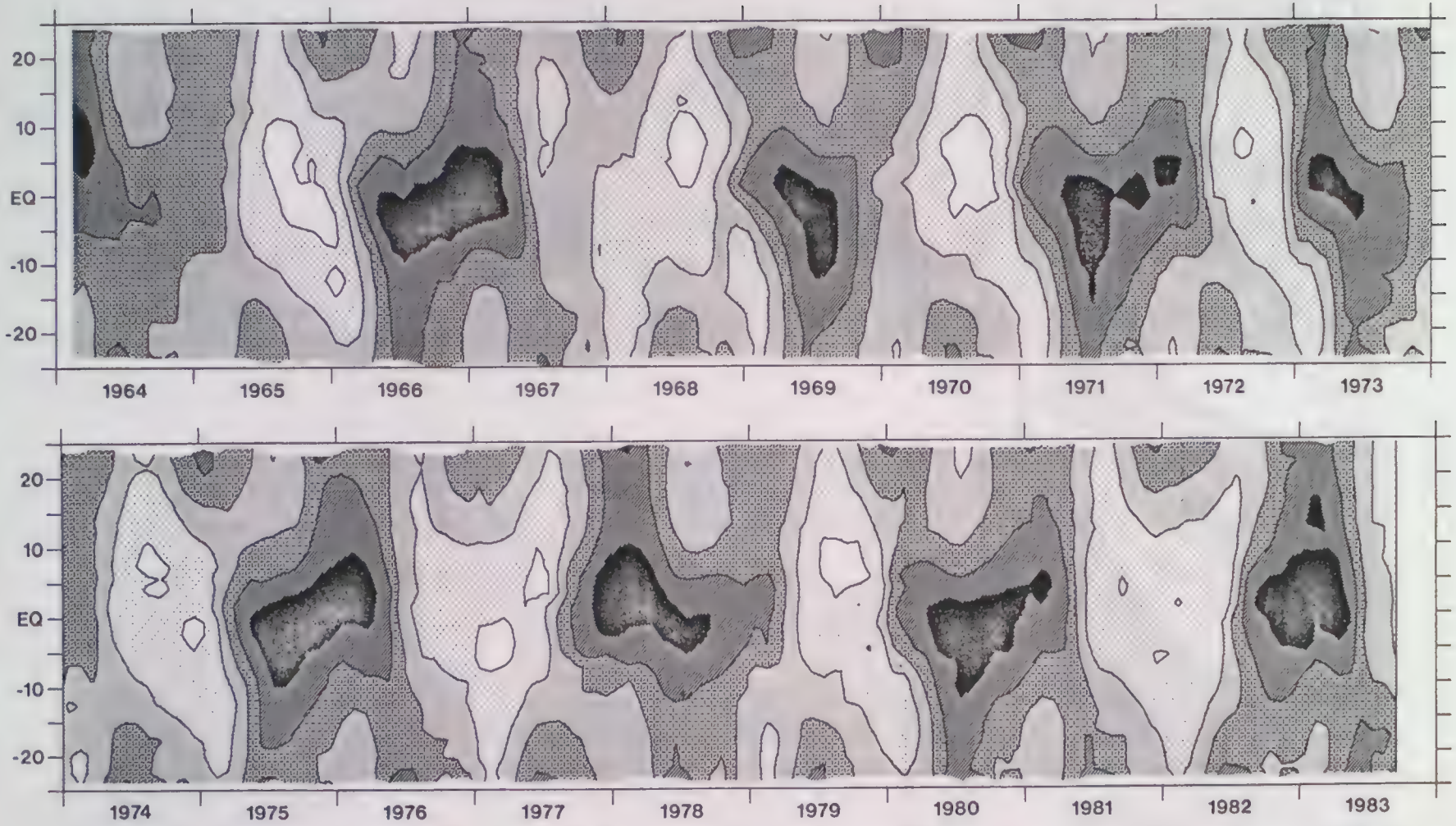


Latitude–time plot of monthly mean zonal wind at 30 mb. Shading interval is 10 m $s^{-1}$, proceeding from negative (light) values to positive (dark). White shading is for winds just below −30 m $s^{-1}$, and black indicates winds greater than 10 m $s^{-1}$. Computer plotting utilized a ¼–½–¼ smoothing in both latitude and time. (The zero wind line is the outer boundary of the diagonally striped region.)

Figure 6.30. From Dunkerton and Delisi (1985).

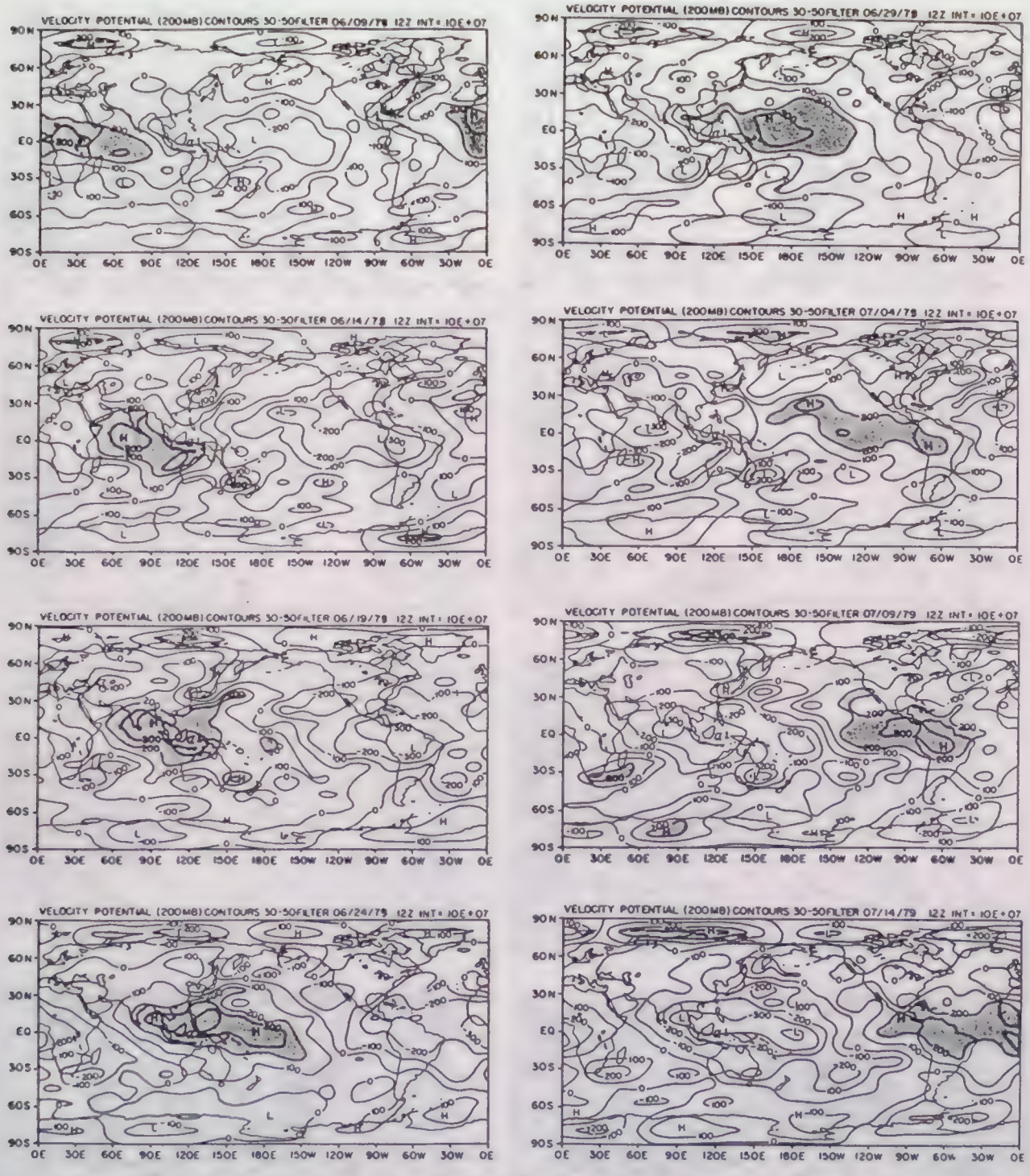


Velocity potential at 200 mb over the globe on the time scale of 30 to 50 days. The maps shown here cover the period 9 June through 14 July 1979 at intervals of 5 days. The isopleths are drawn at an interval of $100 \times 10^4$ m$^2$ s$^{-1}$. The shaded area shows values larger than $200 \times 10^4$ units. These are a subset of maps from the entire year of data.

Figure 6.31. From Krishnamurti et al (1985).

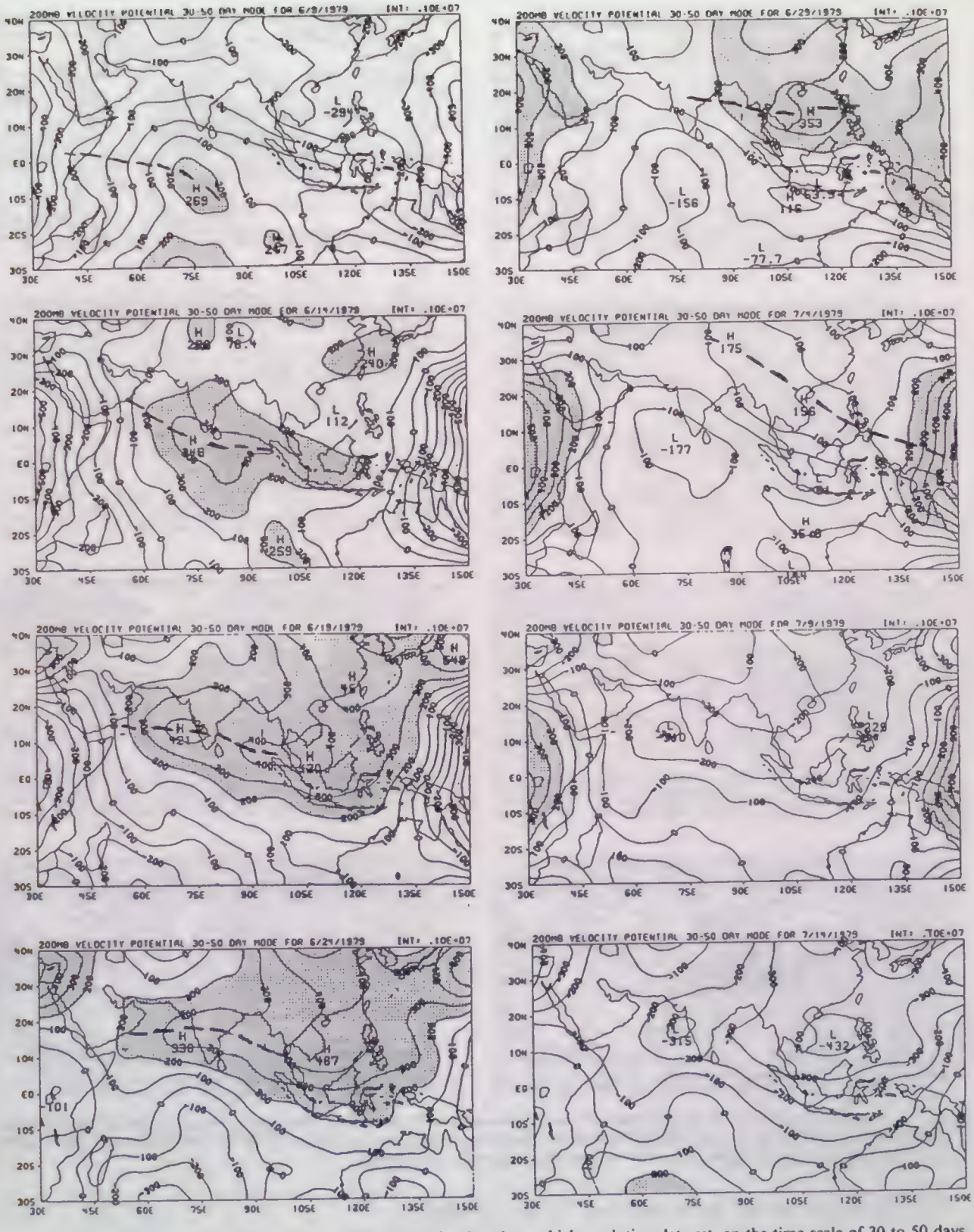


Velocity potential at 200 mb, for the MONEX region based on a high resolution data set, on the time scale of 30 to 50 days. The maps shown here cover the period 9 June through 14 July 1979 at intervals of 5 days. The isopleths are drawn at an interval of 100 $\times 10^4$ m$^2$ s$^{-1}$. The shaded area shows values larger than 200 $\times 10^4$. These are a subset of maps from the entire year of data.

Figure 6.32. From Krishnamurti et al (1985).

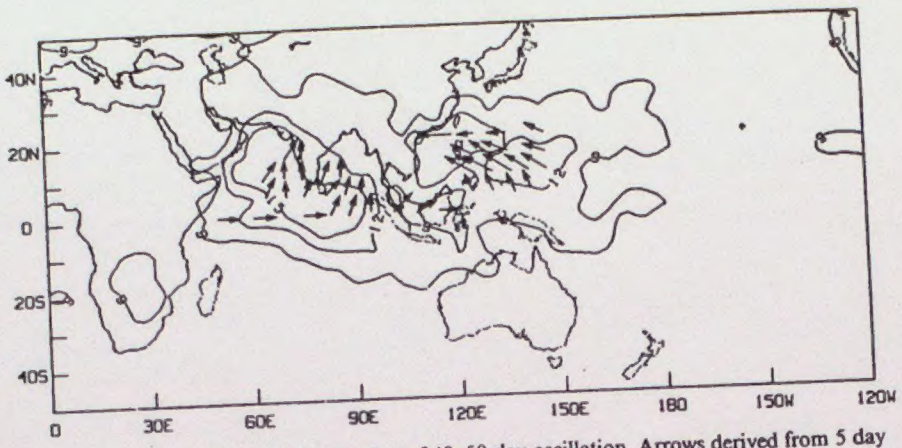


Percentage variance distribution of 40–50 day oscillation. Arrows derived from 5 day lag correlations indicate tendencies of OLR anomaly propagation.

Figure 6.33. From Lau and Chan (1986).

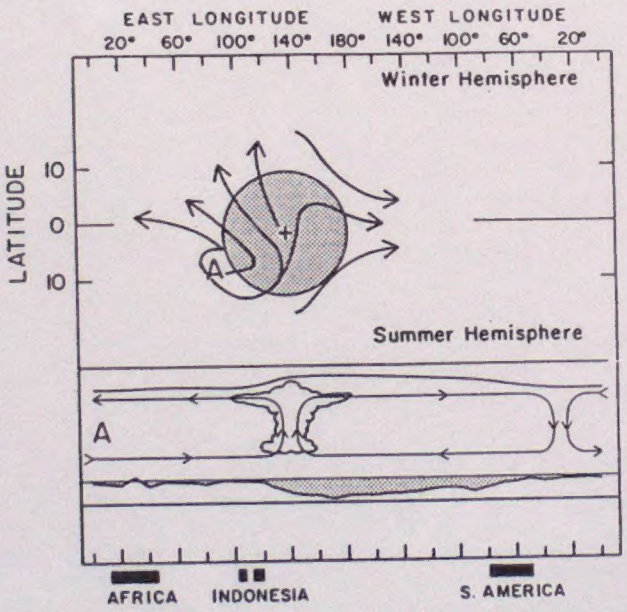


Schematic depiction of the structure of the 40–50 day oscillation at a time of large amplitude. The lower panel represents the structure in the equatorial plane. Shading at the bottom represents the negative pressure anomalies. The line at the top of the lower panel represents the tropopause. The upper panel is a plan view of the disturbance in the upper troposphere. The shaded area there corresponds to a positive anomaly in convection that is centered in the summer hemisphere.

Figure 6.34. From Madden(1986).

## INDEX TO LONG-RANGE FORECASTING AND CLIMATE RESEARCH SERIES

1) THE CLIMATE OF THE WORLD - Introduction and description of world climate.
by C K Folland (March 1986)

2) THE CLIMATE OF THE WORLD - Forcing and feedback processess.
by C K Folland (March 1986)

3) THE CLIMATE OF THE WORLD - El Nino/Southern Oscillation and the Quasi-biennial Oscillation.
by C K Folland (March 1986)

4) THE CLIMATE OF THE WORLD - Climate change: the ancient earth to the 'Little Ice Age'.
by C K Folland

5) THE CLIMATE OF THE WORLD - Climate change: the instumental period.
by C K Folland (March 1986)

6) THE CLIMATE OF THE WORLD - Carbon dioxide and climate (with appendix on simple climate models).
by C K Folland (March 1986)

7a) Sahel rainfall, Northern Hempishere circulation anomalies and worldwide sea temperature changes, (To be published in the Proceedings of the "Pontifical Academy of Sciences Study Week", Vatican, 23-27 September 1986).
by C K Folland, D E Parker, M N Ward and A W Colman (September 1986) (Amended July 1987)

8) Lagged-average forecast experiments with a 5-level general circulation model.
by J M Murphy (March 1986)

9) Statistical Aspects of Ensemble Forecasts.
by J M Murphy (July 1986)

10) The impact of El Nino on an Ensemble of Extended-Range Forecasts. (Submitted to Monthly Weather Review)
by J A Owen and T N Palmer (December 1986)

11) An experimental forecast of the 1987 rainfall in the Northern Nordeste region of Brazil.
by M N Ward, S Brooks and C K Folland (March 1987)

12) The sensitivity of Estimates of Trends of Global and Hemispheric Marine Temperature to Limitations in Geographical Coverage.
by D E Parker (April 1987)

13) General circulation model simulations using cloud distributions from the GAPOD satellite data archive and other sources.
by R Swinbank (May 1987)

14) Similation of the Madden and Julian Oscillation in GCM Experiments.
by R Swinbank (May 1987)

15) Numerical simulation of seasonal Sahel rainfall in four past years using observed sea surface temperatures.
by J A Owen, C K Folland and M Bottomley (April 1988)

16) Not used

17) A note on the use of Voluntary Observing Fleet Data to estimate air-sea fluxes.
by D E Parker (April 1988)

18) Extended-range prediction experiments using an 11-level GCM
by J M Murphy and A Dickinson (April 1988)

19) Numerical models of the Raingauge Exposure problems - field experiments and an improved collector design.
by C K Folland (May 1988)

20) An interim analysis of the leading covariance eigenvectors of worldwide sea surface temperature anomalies for 1901-80.
by C K Folland and A Colman (April 1988)

21) Prospects for long range forecasting for the United Kingdom.
by A Dickinson and C K Folland (July 1988)

22) CLIMATE OF THE WORLD (Restricted Issue) 1. Introduction to world climate

2. Description of world climate
by C K Folland and D E Parker (July 1988)

23) CLIMATE OF THE WORLD (Restricted issue) 3. Climatic forcing and feedback processes.
I. Forcing from above.

4. Climatic forcing and feedback processes.
II. Interactions with land surface
by C K Folland and D E Parker (July 1988)

24) CLIMATE OF THE WORLD (Restricted Issue) 5. Ocean-atmosphere interaction
by D E Parker and C K Folland (July 1988)

25) CLIMATE OF THE WORLD (Restricted Issue) 6. The El Nino/Southern Oscillation, the Quasi-Biennial Oscillation, and the 30-60 day variations.
by C K Folland and D E Parker (July 1988)

26) CLIMATE OF THE WORLD (Restricted Issue) 7. A review of palaeoclimate from the early Earth to the Pleistocene ice ages

8. Climate from the late glacial to the "Little ice age"
by C K Folland and D E Parker (July 1988)

27) CLIMATE OF THE WORLD 9. Climatic change in the instrumental period
(Restricted Issue) by D E Parker and C K Folland (July 1988)

28) CLIMATE OF THE WORLD 10. Carbon dioxide and other greenhouse gases, and
(Restricted Issue) climatic variation
(with appendix on simple climate models).
by D E Parker, C K Folland and D J Carson
(July 1988)